AD-A047 396 SCIENCE APPLICATIONS INC BERKELEY CALIF F/G 20/14
SELECTED TOPICS IN TRANSMISSION-LINE THEORY FOR EMP INTERNAL IN--ETC(U)
AUG 77 F M TESCHE, T K LIU F29601-76-C-0125

UNCLASSIFIED AFWL-TR-77-73 NL

OF 2
AD A047396

AFWL-TR-77-73

AD-E200 044
AFWL-TR-
77-73

SELECTED TOPICS IN TRANSMISSION-LINE THEORY FOR EMP INTERNAL INTERACTION PROBLEMS

Science Applications, Inc.
Berkeley, CA 94701

August 1977

Final Report

Approved for public release; distribution unlimited

AIR FORCE WEAPONS LABORATORY
Air Force Systems Command
Kirtland Air Force Base, NM 87117

This final report was prepared by Science Applications, Inc., Berkeley, California, under Contract F29601-76-C-0125, Job Order 12090513 with the Air Force Weapons Laboratory, Kirtland Air Force Base, New Mexico. Captain Howard G Hudson (ELP) was the Laboratory Project Officer-in-Charge.

This technical report has been reviewed and is approved for publication.

HOWARD G. HUDSON
Captain, USAF
Project Officer

FOR THE COMMANDER

AARON B. LOGGINS
Lt Colonel, USAF
Chief, Phenomenology & Technology Branch

JAMES L. GRIGGS, JR.
Colonel, USAF
Chief, Electronics Division

This report has been reviewed by the Office of Information (OI) and is releasable to the National Technical Information Service (NTIS). At NTIS, it will be available to the general public, including foreign nations.

DO NOT RETURN THIS COPY. RETAIN OR DESTROY

UNCLASSIFIED

SECURITY CLASSIFICATION OF THIS PAGE (When Data Entered)

REPORT DOCUMENTATION PAGE

READ INSTRUCTIONS BEFORE COMPLETING FORM

1. REPORT NUMBER: AFWL-TR-77-73
2. GOVT ACCESSION NO.:
3. RECIPIENT'S CATALOG NUMBER:
4. TITLE (and Subtitle): SELECTED TOPICS IN TRANSMISSION-LINE THEORY FOR EMP INTERNAL INTERACTION PROBLEMS.
5. TYPE OF REPORT & PERIOD COVERED: Final Report.
6. PERFORMING ORG. REPORT NUMBER:
7. AUTHOR(s): F. M. Tesche, T. K. Liu
8. CONTRACT OR GRANT NUMBER(s): F29601-76-C-0125
9. PERFORMING ORGANIZATION NAME AND ADDRESS: Science Applications, Inc., Berkeley, CA 94701
10. PROGRAM ELEMENT, PROJECT, TASK AREA & WORK UNIT NUMBERS: 64747F, 12090513, 05
11. CONTROLLING OFFICE NAME AND ADDRESS: Air Force Weapons Laboratory (ELP), Kirtland Air Force Base, NM 87117
12. REPORT DATE: Aug[redacted]77
13. NUMBER OF PAGES: 98 (101 p.)
14. MONITORING AGENCY NAME & ADDRESS (if different from Controlling Office):
15. SECURITY CLASS. (of this report): UNCLASSIFIED
15a. DECLASSIFICATION/ DOWNGRADING SCHEDULE:
16. DISTRIBUTION STATEMENT (of this Report): Approved for public release; distribution unlimited.

18. AFWL, SBIE

19. TR-77-73, AD-E201 044

17. DISTRIBUTION STATEMENT (of the abstract entered in Block 20, if different from Report)

409694

18. SUPPLEMENTARY NOTES

19. KEY WORDS (Continue on reverse side if necessary and identify by block number)

Transmission Lines
Single-Wire transmission line
Capacitance
Electromagnetic Pulse (EMP) Coupling to Transmission Lines

20. ABSTRACT (Continue on reverse side if necessary and identify by block number)

This report discusses a number of modifications of a single wire transmission line model for use in EMP internal interaction studies. The importance of including the effects of local line perturbations (such as a cable clamp) is discussed in terms of the reflection coefficient presented to waves on the transmission line, and general curves for determining when to neglect such effects are given. Next, the behavior of a finite length transmission line with periodic loading is investigated and results are compared with those of an infinite line

(over)

next page

DD FORM 1 JAN 73 1473 EDITION OF 1 NOV 65 IS OBSOLETE

UNCLASSIFIED

SECURITY CLASSIFICATION OF THIS PAGE (When Data Entered)

20. ABSTRACT (Cont'd)

using Floquet's theorem. Finally, the bulk current response of a general multiconductor transmission is related to the current on a single wire line and a prescription for determining an equivalent single wire characteristic impedance and a load impedance from the multiconductor quantities is described.

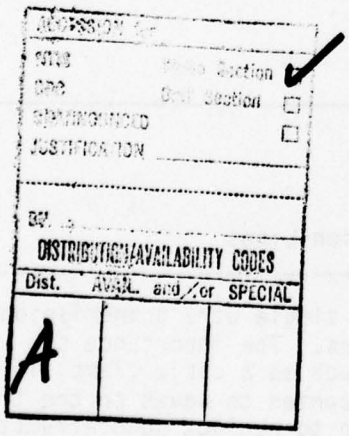

TABLE OF CONTENTS

LIST OF FIGURES

SECTION I

INTRODUCTION

The calculation of the propagation and distribution of transient electromagnetic energy within the internal regions of aircraft and missiles frequently employs transmission line theory. As outlined in other reports (refs. 1,2,3) solutions using this method often involve the assumptions of having only a single conductor transmission line instead of a multiconductor line, of considering only TEM modes of propagation on the line, and of having a uniform transmission line.

As indicated in ref. (2), a number of improvements can be made to increase the modeling accuracy for treating these problems found in the area of electromagnetic pulse (EMP) internal interaction. One general class of improvements consists of adding a tee network of lumped, passive elements to an otherwise uniform transmission line, so as to account for a perturbation in the local transmission line geometry.

---

1. Tesche, F.M., et al., "Internal Interaction Analysis: Topological Concepts and Needed Model Improvements," AFWL-TR-75-282, Air Force Weapons Laboratory, Kirtland Air Force Base, NM, October 1975.

2. Tesche, F.M., et al., "Evaluation of Present Internal EMP Interaction Technology: Description of Needed Improvements," AFWL-TR-75-288, Air Force Weapons Laboratory, Kirtland Air Force Base, NM, October 1975.

3. Boeing Aircraft Corporation, "Common Mode Model Development for Complex Cable Systems," Boeing Report D224-10015-4, June 19, 1973.

Using this approach, an equivalent tee circuit for a single cable clamp on a transmission line has been developed in ref. (4). Other "canonical" problems which have been recently investigated include a cable passing over a thin septum (ref. 5), a cable passing near a hole in the ground plane (ref. 6), and a cable with a sharp bend (ref. 7).

An investigation of actual aircraft cable layouts shows that there is often more than just one perturbation to a transmission line. Many times, multiple loading of a transmission line will occur in a periodic fashion, as in a transmission line passing over a series of ribs within the aircraft, or for a line fastened periodically to a metallic wall by cable clamps. In a recent report (ref. 8), Lam investigated the behavior of a cable passing

---

4. Tesche, F.M., and T.K. Liu, "An Electric Model for a Cable Clamp on a Single Wire Transmission Line," AFWL-TR-76-325, Air Force Weapons Laboratory, Kirtland Air Force Base, NM, December 1976.

5. Coen, S., T.K. Liu and F.M. Tesche, "Calculation of the Equivalent Capacitance of a Rib near a Single-Wire Transmission Line," AFWL-TR-77-60, Air Force Weapons Laboratory, Kirtland Air Force Base, NM, February 1977.

6. Lee, K.S.H., and F.C. Yang, "A Wire Passing by a Circular Aperture in an Infinite Ground Plane," AFWL-TR-77- , Air Force Weapons Laboratory, Kirtland Air Force Base, NM, Febraury 1977.

7. Lam, J., "Equivalent Lumped Parameters for a Bend in a Two-Wire Transmission Line," AFWL-TR-77-5, Air Force Weapons Laboratory, Kirtland Air Force Base, NM, January 1977.

8. Lam, J., "Propagation Characteristics of a Periodically Loaded Transmission Line," AFWL-TR-76-324, Air Force Weapons Laboratory, Kirtland Air Force Base, NM, December 1976.

over periodic obstacles using Floquet's theorem. By postulating an infinite transmission line loaded at regular intervals with identical, symmetrical tee sections, the dispersion relation for determining the wave propagation was developed. This leads to various relations for the propagation constant, pass and stop bands, and phase and group velocity on the line.

Aircraft cables, however, rarely occur as a single wire transmission line. Usually they are multiconductor cables with a wide variety of loads. Nevertheless, such cables are often modeled as a single wire transmission line with an "appropriate" load impedance. The choice of the best load impedance for the single wire model is an important consideration for the use of this simplified internal interaction analysis technique.

This report investigates these various topics and their importance in EMP analysis. Section II suggests a technique for determining when the effects of an isolated perturbation along a single wire transmission line can be ignored and when it must be considered in the analysis of transient currents flowing on the line. Section III goes on to consider the effects of more than one obstacle which is periodically positioned along the line. Unlike the analysis of ref. (8), however, we consider a finite number of

periodic obstacles and compare results with those obtained by Floquet's theorem.

Section IV discusses general multiconductor transmission line theory and the relation between the total or "bulk" current on a multiconductor line and the current flowing on a single conductor line having suitably chosen loads and characteristic impedance. Specific formulae are presented for determining these quantities for an aribtrary multiconductor line, and a number of examples are given.

SECTION II

IMPORTANCE OF EFFECTS OF PERTURBING OBSTACLES

As described in refs. (4) through (8), the effects of a localized discontinuity in an otherwise uniform transmission line can be represented by a tee network of lumped, passive elements inserted in the transmission line. As an example, consider a single wire line over a ground plane and passing near an electrically small obstacle, as in Figure 1. Figure 2 illustrates the transmission line model for this case, with the obstacle effects represented by the capacitance and inductance elements of the tee network.

In applying the results of the canonical problems to a single line model of aircraft wiring, it is often useful to estimate the overall effect of a particular line perturbation before carrying out a complete transient analysis of the transmission line. If a particular line perturbation will only marginally affect the response at a load, then it need not be considered in the transmission line model.

One measure of the importance of a line perturbation is the reflection coefficient, ρ. This quantity is defined as

$$\rho = \frac{V^-}{V^+}$$

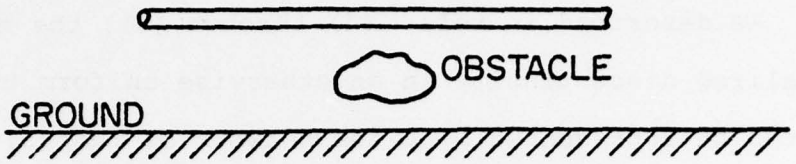

Figure 1. Uniform Transmission Line Passing Near Obstacle

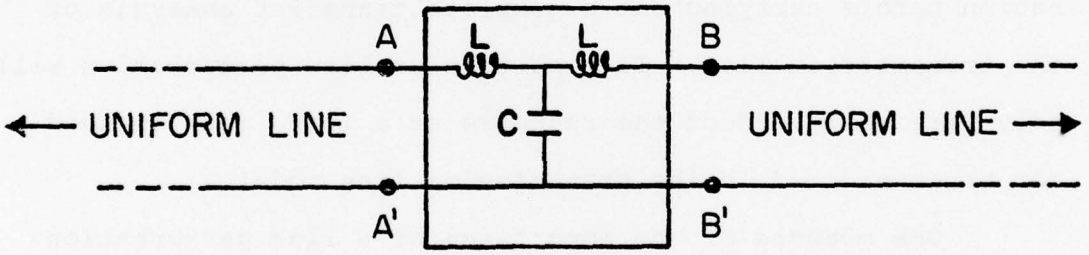

Figure 2. Two-Port Network Representing Effect of Obstacle

where V^- is the reflected voltage wave (propagating to the left of A-A' in Figure 2) and V^+ is the incident voltage wave. Of particular interest is the reflection coefficient ρ at the terminals A-A' of the equivalent two-port network representing the perturbing obstacle.

The reflection coefficient at A-A' will depend upon the termination impedance of the line to the right of terminals B-B' . However, since we are interested in the effects of perturbing obstacle alone, it is convenient to assume that the line connected to B-B' is perfectly matched. In this manner, the reflection coefficient at A-A' will depend only on the obstacle parameters, the line characteristic impedance, and the operating radian frequency ω.

As is well known (ref. 9), the reflection coefficient at A-A' can be expressed as

$$\rho = \frac{Z_L - Z_C}{Z_L + Z_C} \qquad (1)$$

where Z_C is the characteristic impedance of the transmission line, and Z_L is the load impedance presented by the circuit and transmission line to the right of A-A'.

Since the line to the right of B-B' is assumed to be matched, the load impedance Z_L can be computed by

9. Ramo, S., and J. Whinnery, Fields and Waves in Modern Radio, John Wiley & Sons, New York, 1964.

considering the circuit shown in Figure 3. Using $s = \sigma + j\omega$ for the complex frequency, where $j = \sqrt{-1}$, elementary circuit analysis shows that the impedance at terminals A-A' is

$$Z_L(s) = \frac{s^3L^2C + s^2LCZ_c + 2sL + Z_c}{s^2LC + sCZ_c + 1} \tag{2}$$

It is convenient to introduce a normalized frequency p and a normalized impedance ξ as

$$p = s\sqrt{LC} \tag{3}$$

and

$$\xi = \sqrt{\frac{L}{C}}\ \frac{1}{Z_c} \tag{4}$$

so as to simplify Equation (2). In this manner, the impedance can be written as

$$Z_L(p) = Z_c\ \frac{p^3\xi + p^2 + 2p\xi + 1}{p^2 + p/\xi + 1} \tag{5}$$

By inserting Equation (5) into Equation (1) and simplifying, the reflection coefficient becomes

$$\rho = \frac{p\xi(p^2 + 2 - 1/\xi^2)}{p^2(p\xi+2) + p(2\xi+1/\xi) + 2} \tag{6}$$

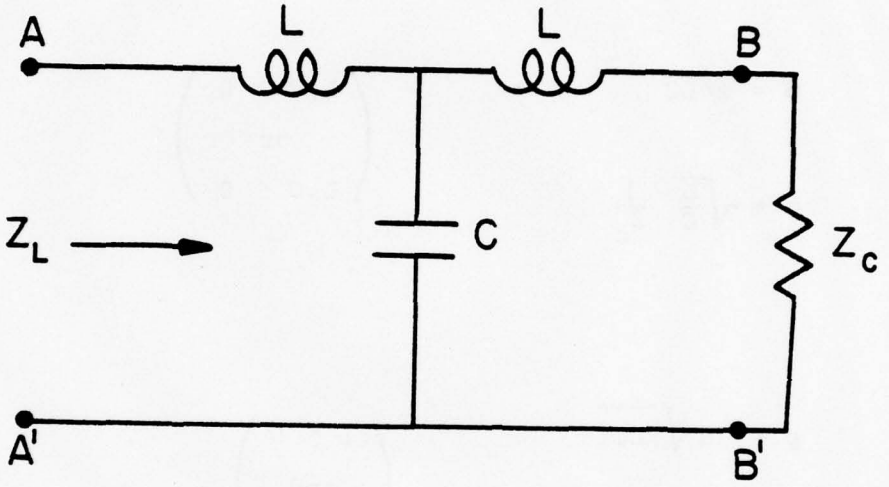

Figure 3. Impedance at A-A' Presented by Equivalent Tee Network Loaded by Infinite Transmission Line at B-B'.

It is important to realize that the values of L and C in the equivalent tee circuit for the obstacle may be positive or negative quantities. Thus, care must be used in evaluating Equations (3) and (4) for p and ξ. It may be seen that the following sets of values for p and ξ must be used in evaluating Equation (6):

$$p = s\sqrt{LC} \qquad \begin{pmatrix} L,C > 0 \\ \text{or} \\ L,C < 0 \end{pmatrix}$$

$$\xi = \sqrt{\frac{L}{C}}\ \frac{1}{Z_c}$$

or

$$p = js\sqrt{|LC|} \qquad \begin{pmatrix} L < 0 \\ \text{and} \\ C > 0 \end{pmatrix}$$

$$\xi = j\sqrt{\left|\frac{L}{C}\right|}$$

or

$$p = js\sqrt{|LC|} \qquad \begin{pmatrix} L > 0 \\ \text{and} \\ C < 0 \end{pmatrix}$$

$$\xi = -j\sqrt{\left|\frac{L}{C}\right|}\ \frac{1}{Z_c}$$

The behavior of ρ as a function of frequency for a specific set of obstacle parameters L and C gives an indication of the importance of the obstacle interaction on the transmission behavior. If, for example, the magnitude of ρ is very small for a particular L and C over a specified range, the obstacle could be neglected in the transmission line model.

For the case of L and C both positive or negative, Figure 4 shows a plot of the magnitude of the reflection coefficient from Equation (6) as a function of the normalized frequency, $p=\omega\sqrt{LC}$, for various values of ξ. It can be noted from Equation (6) that there is a zero in the reflection coefficient at the frequency

$$p_o = \pm \sqrt{1/\xi^2 - 2} \qquad (7)$$

When $\xi < \sqrt{2}/2$, this zero is real, occurring on the σ axis in the complex frequency plane. For $\xi > \sqrt{2}/2$, however, the zero is imaginary and is located along the $j\omega$ axis. Thus, we expect the curves of $|\rho|$ for $\xi > 0.707...$ to be substantially different from those for $|\rho|$ presented in Figure 4.

Figure 5 shows the magnitude of the reflection coefficient vs. normalized frequency for various $\xi > 0.707....$

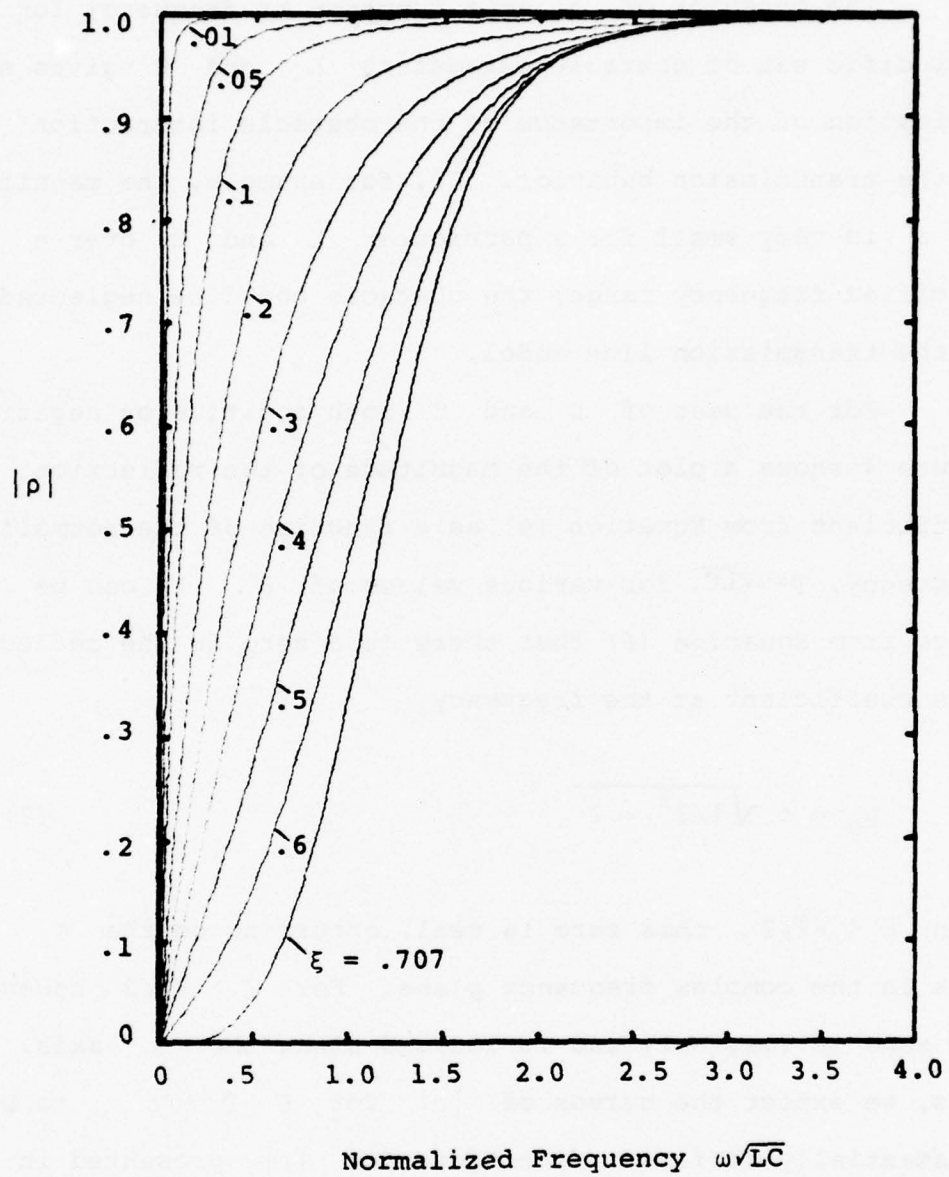

Figure 4. Plot of Reflection Coefficient Magnitude vs. Normalized Frequency for $\xi \leq 0.707$. (L and C both have same sign.)

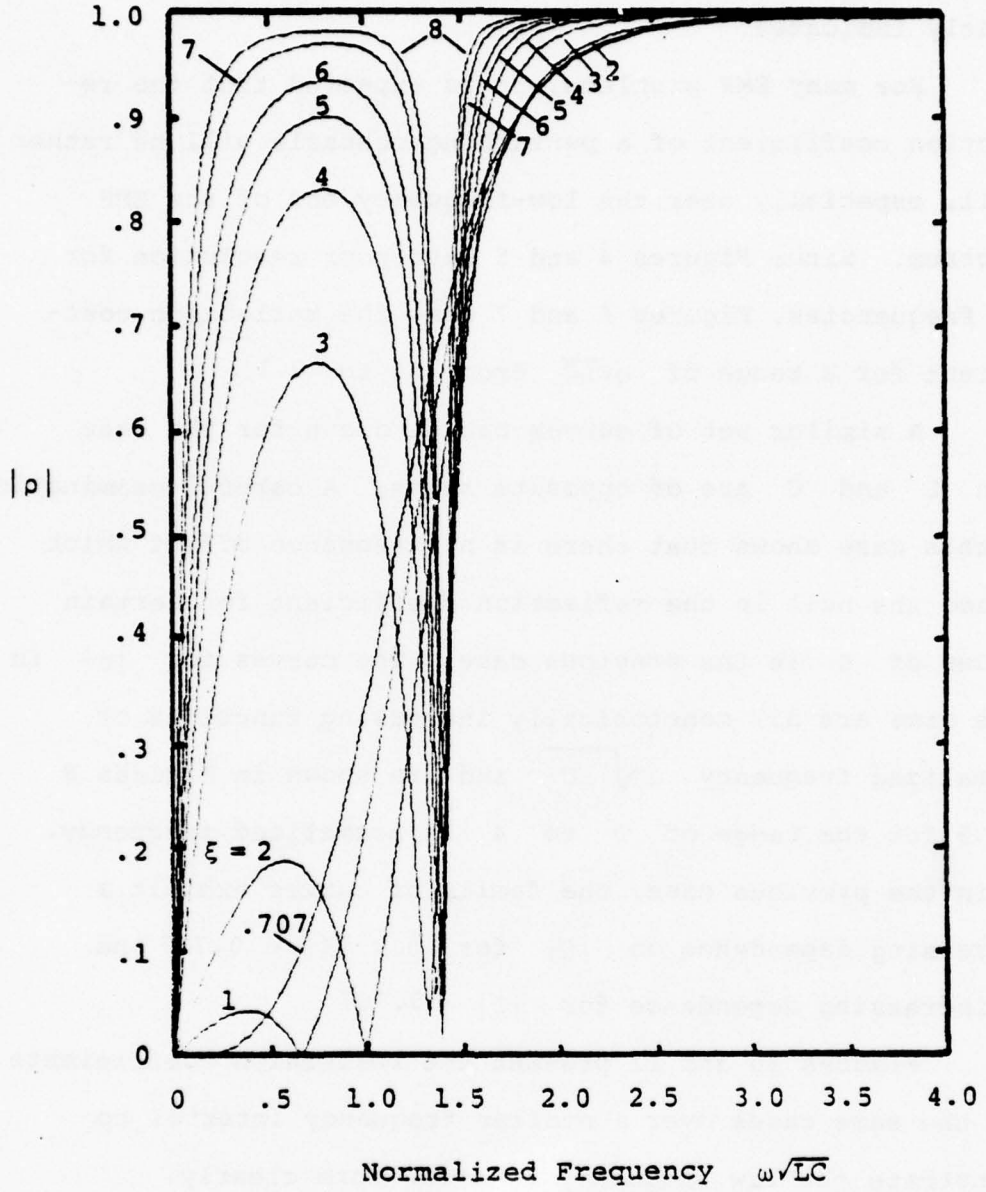

Figure 5. Plot of Reflection Coefficient Magnitude vs. Normalized Frequency for $\xi \geq 0.707$.
(L and C both have same sign.)

The effect of the zero in the reflection coefficient is clearly indicated.

For many EMP problems, it is expected that the reflection coefficient of a perturbing obstacle will be rather small, especially near the low-frequency end of the EMP spectrum. Since Figures 4 and 5 have poor resolution for low frequencies, Figures 6 and 7 show the reflection coefficient for a range of $\omega\sqrt{LC}$ from 0 to 0.1 .

A similar set of curves can be drawn for the case when L and C are of opposite signs. A careful examination of this case shows that there is no resonance effect which caused the null in the reflection coefficient for certain values of ξ in the previous case. The curves for $|\rho|$ in this case are all monotonically increasing functions of normalized frequency $\omega\sqrt{|LC|}$ and are shown in Figures 8 and 9 for the range of 0 to 4 in normalized frequency. As in the previous case, the family of curves exhibit a decreasing dependence on $|\xi|$ for $0 < |\xi| < 0.707$ and an increasing dependence for $|\xi| > 0.707$.

Figures 10 and 11 present the reflection coefficients for the same cases over a smaller frequency interval to illustrate the low frequency behavior more clearly.

In some instances, it may be expected that an obstacle will present a strong capacitive discontinuity to the

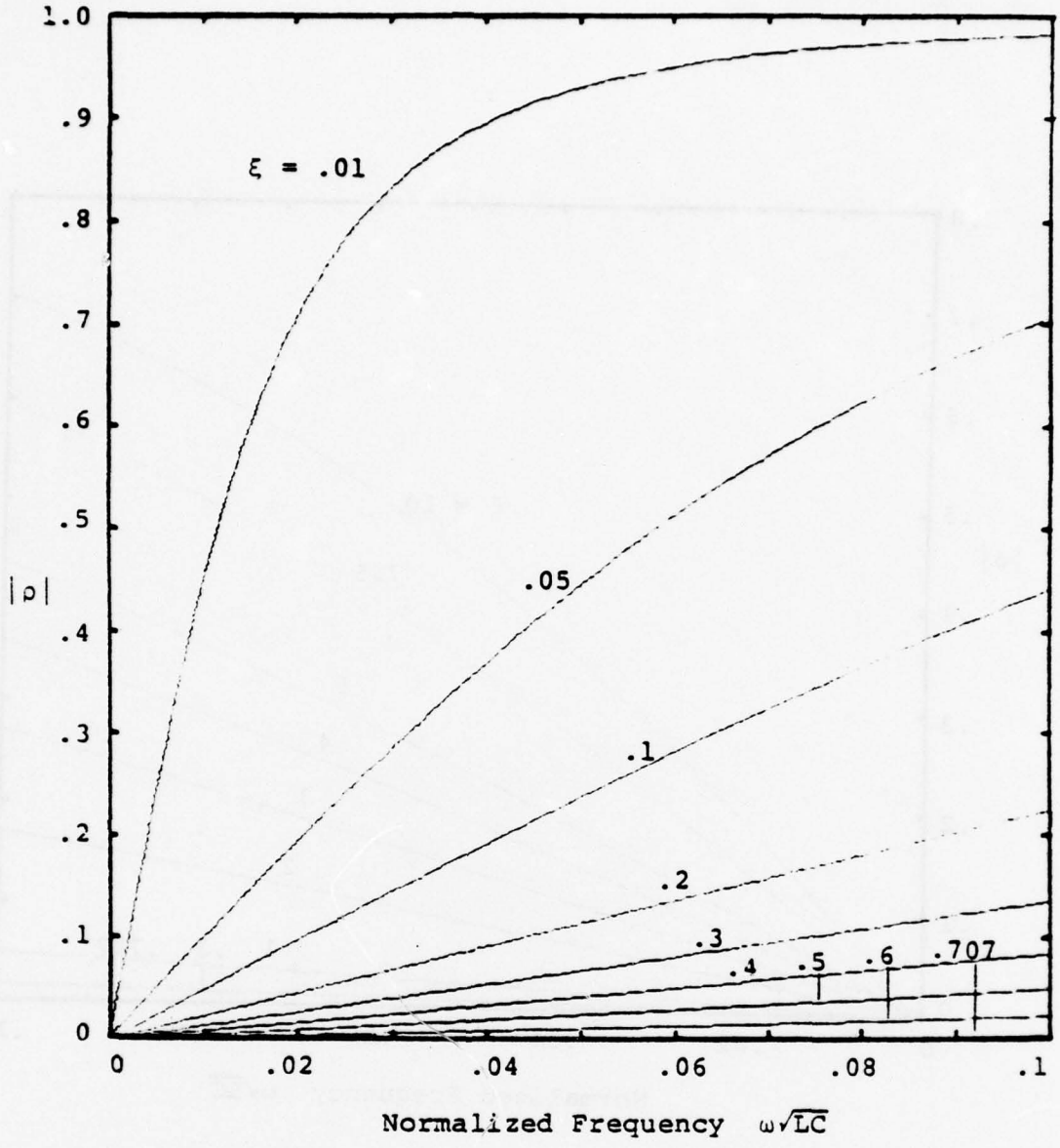

Figure 6. Expanded Plot of Reflection Coefficient Magnitude vs. Normalized Frequency for $\xi \leq 0.707$.
(L and C both have the same sign.)

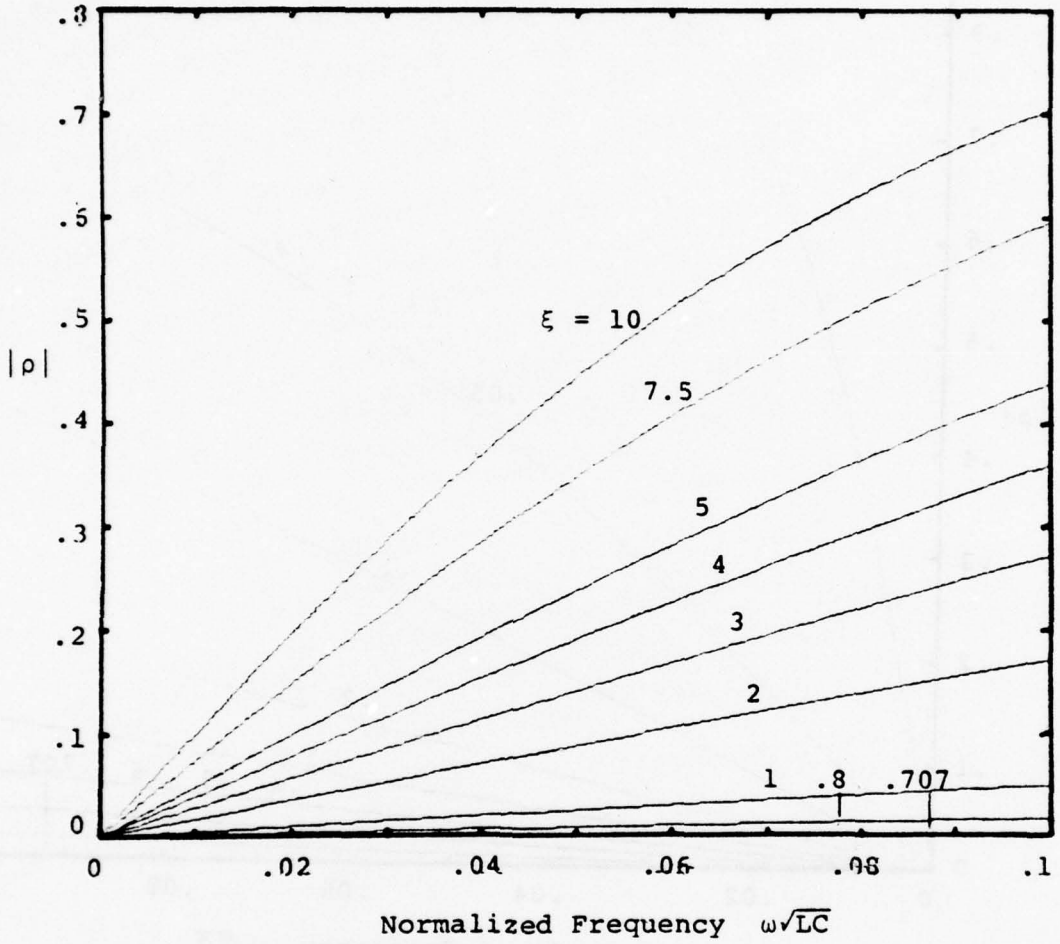

Figure 7. Expanded Plot of Reflection Coefficient Magnitude vs. Normalized Frequency for $\xi \geq 0.707$.
(L and C both have the same sign.)

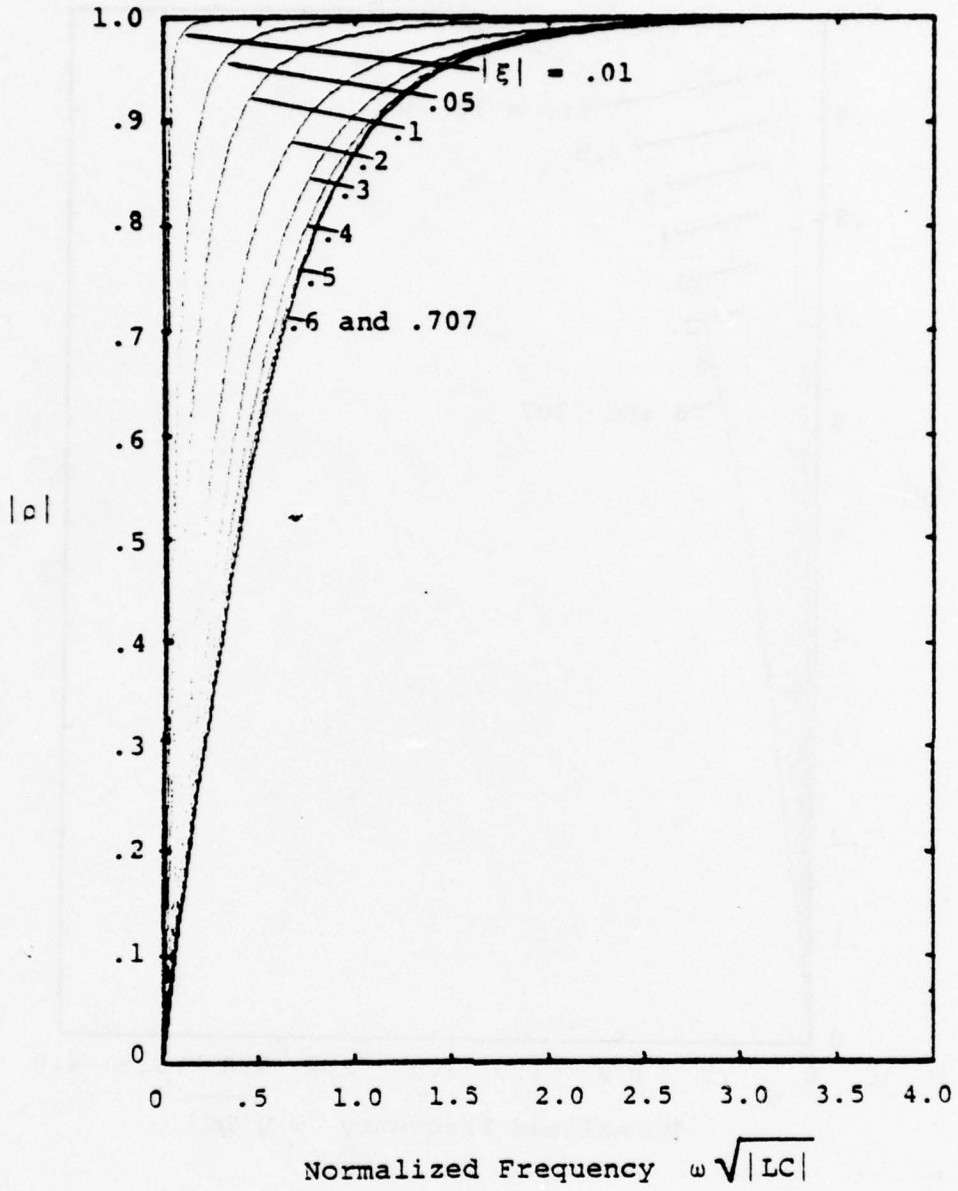

Figure 8. Plot of Reflection Coefficient Magnitude vs. Normalized Frequency for $|\xi| \leq 0.707$.
(L and C have opposite signs.)

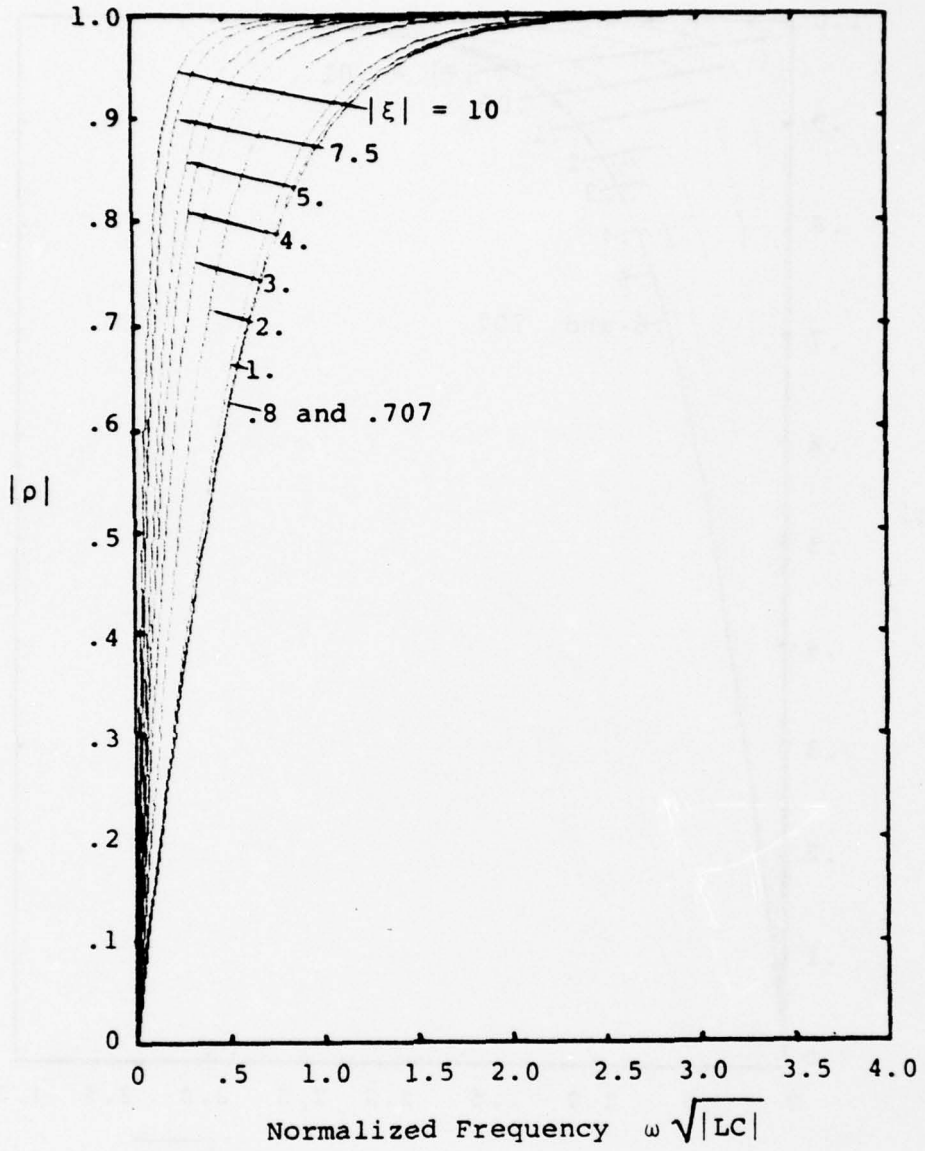

Figure 9. Plot of Reflection Coefficient Magnitude vs. Normalized Frequency for $|\xi| \geq 0.707$.
(L and C have opposite signs.)

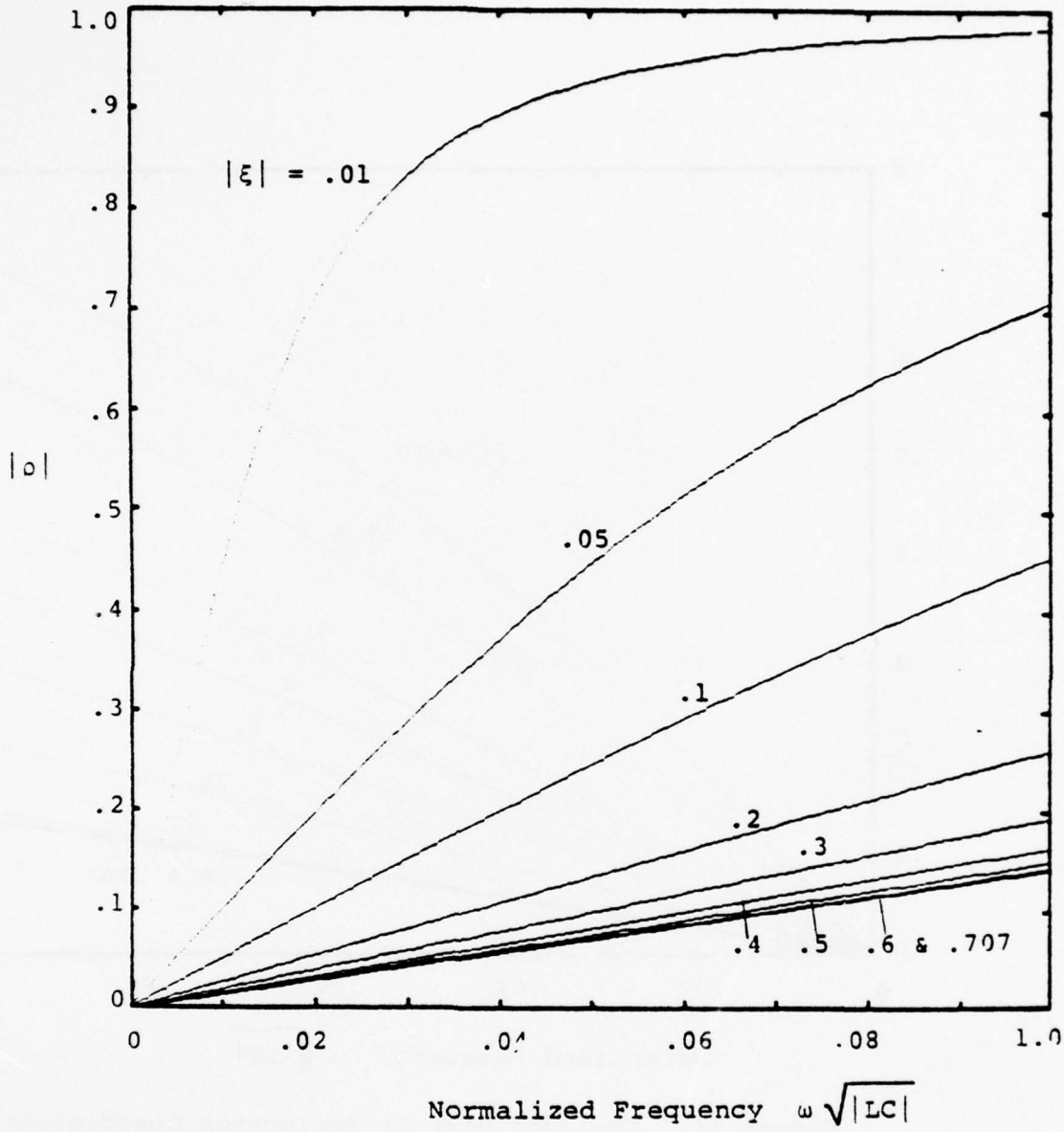

Figure 10. Expanded Plot of Reflection Coefficient Magnitude vs. Normalized Frequency for $|\xi| \leq 0.707$.
(L and C have opposite signs.)

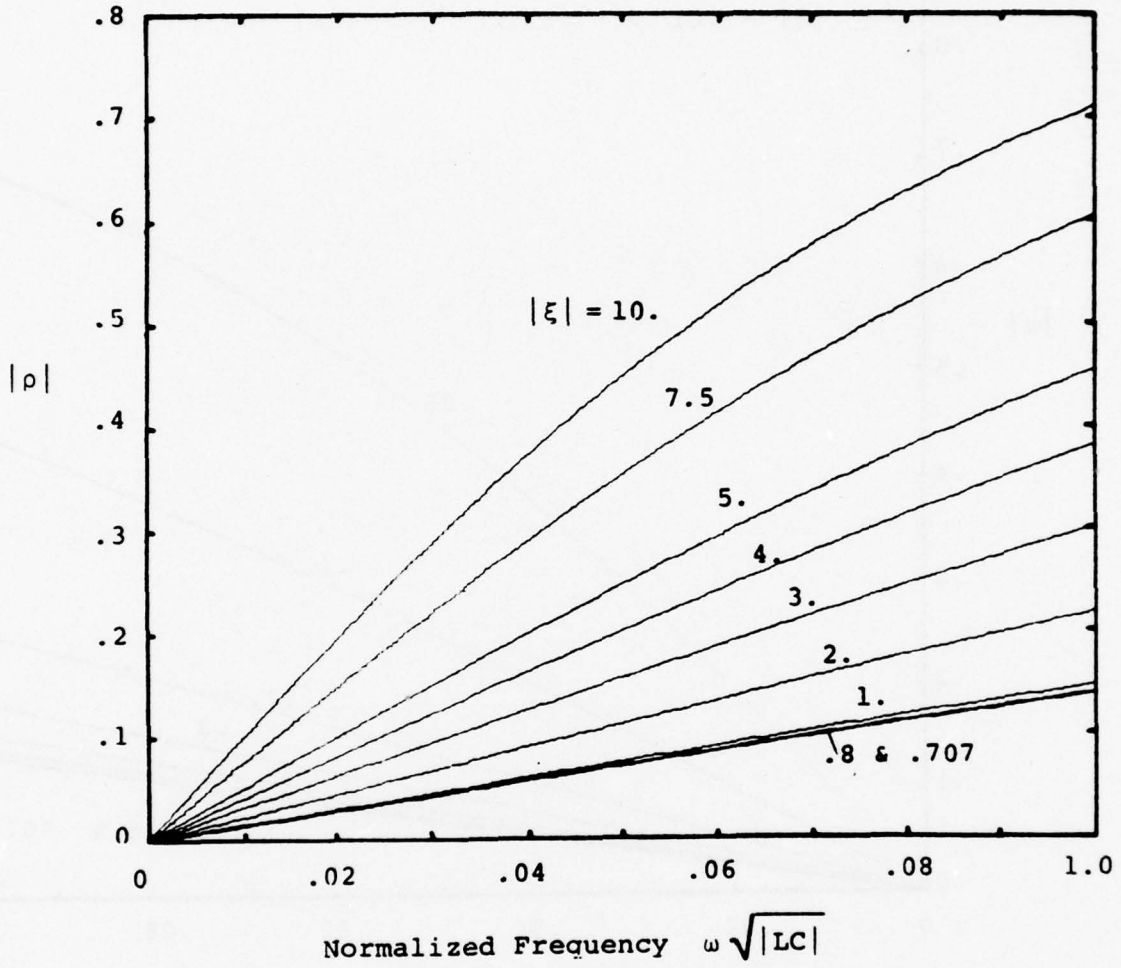

Figure 11. Expanded Plot of Reflection Coefficient Magnitude vs. Normalized Frequency for $|\xi| \geq 0.707$.
(L and C have opposite signs.)

transmission line, with the inductance elements of the two-port network in Figure 2 being either absent or having very small values. Such was the case in ref. (5). Under these circumstances it is difficult to employ Figures 4 through 11 to assess the importance of the obstacle, since the normalized frequency p approaches zero and the normalized impedance approaches either zero or infinity at the same time.

To consider this case, the load impedance at A-A' for zero inductance can be written directly from Equation (2) as

$$Z_L(s) = \frac{Z_c}{sCZ_c + 1} \tag{8}$$

which immediately gives a reflection coefficient from Equation (1) as

$$\rho(s) = - \frac{sCZ_c}{sCZ_c + 2} \tag{9}$$

Defining a new normalized complex frequency s_n as

$$s_n = sCZ_c \tag{10}$$

the reflection coefficient becomes

$$\rho(s_n) = \frac{-s_n}{s_n + 2} \tag{11}$$

In a similar fashion, if the obstacle presents only an inductive discontinuity, the impedance at A-A' is

$$Z_L(s) = Z_c + 2sL \tag{12}$$

and the reflection coefficient becomes

$$\rho(s_n) = \frac{s_n}{s_n + 2} \tag{13}$$

where the complex frequency s_n now takes the value

$$s_n = \frac{sL}{Z_c} \tag{14}$$

Notice that the magnitude of ρ from Equations (11) or (13) is not dependent on the sign of L or C. Moreover, the magnitudes of Equations (11) and (13) are identical. Hence, only one plot of this simple function is presented in Figure 12.

As an example of the use of these curves, suppose that a transmission line with a characteristic impedance $Z_c = 100$ ohms passes near a perturbing obstacle. If the values of inductance and capacitance are found to be $L = 2.5\times10^{-9}$ henrys and $C = 6\times10^{-12}$ farads from the solution of a particular canonical problem, the normalized

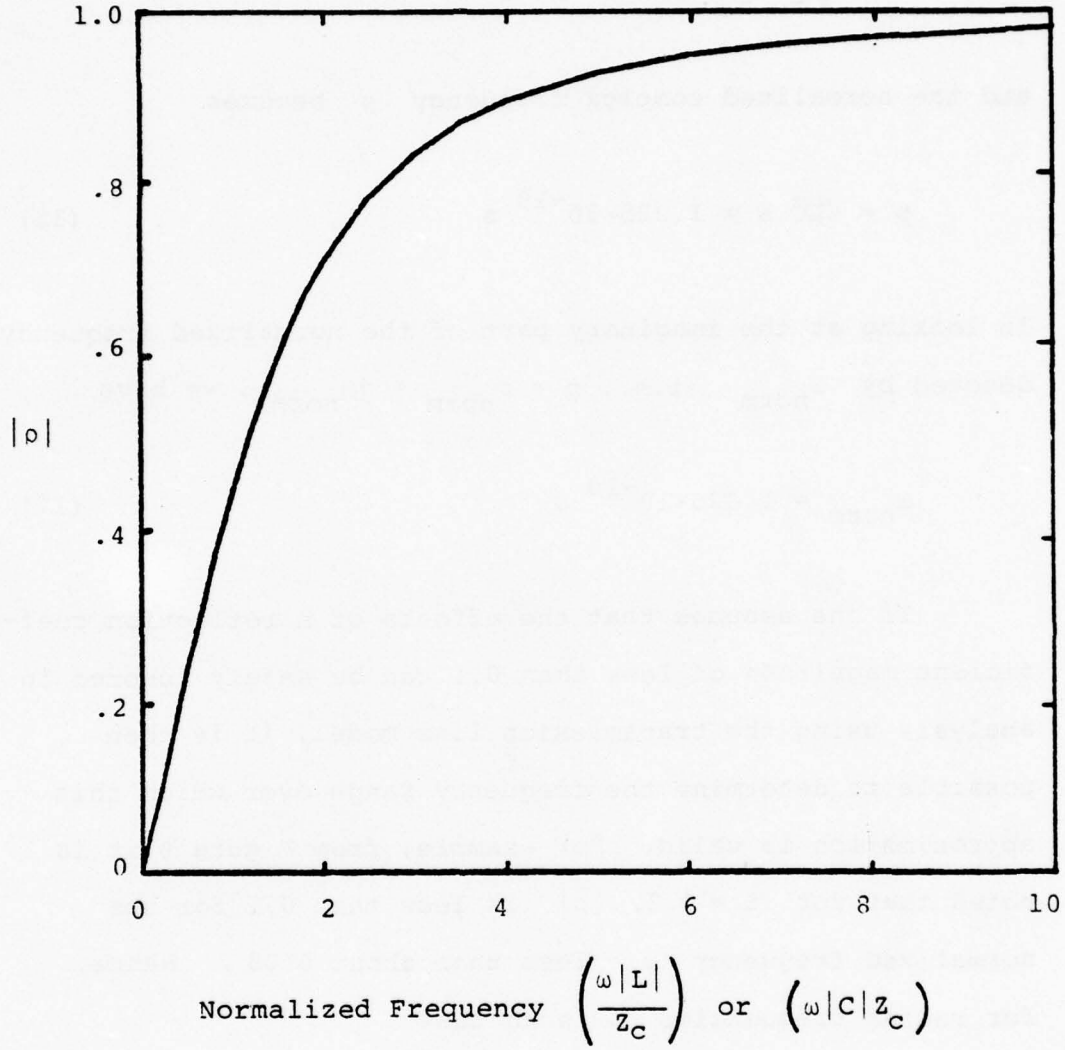

Figure 12. Plot of Reflection Coefficient Magnitude vs. Normalized Frequency for Inductive or Capacitive Discontinuity.

impedance ξ becomes

$$\xi = \sqrt{\frac{L}{C}} \frac{1}{Z_c} = .204 \tag{15}$$

and the normalized complex frequency p becomes

$$p = \sqrt{LC}\, s = 1.225\times10^{-10}\, s \tag{16}$$

In looking at the imaginary part of the normalized frequency, denoted by ω_{norm} (i.e., $p = \sigma_{norm} + j\omega_{norm}$), we have

$$\omega_{norm} = 1.225\times10^{-10}\, \omega \tag{17}$$

If one assumes that the effects of a reflection coefficient magnitude of less than 0.1 can be safely ignored in the analysis using the transmission line model, it is then possible to determine the frequency range over which this approximation is valid. For example, from Figure 6 it is noted that for $\xi = 0.2$, $|\rho|$ is less than 0.1 for the normalized frequency ω_n less than about 0.05 . Hence, for radian frequencies ω such that

$$\omega < \frac{.05}{1.225\times10^{-10}} = 4.08\times10^{8} \text{ rad/sec}$$

or frequencies f so that

$$f < 64.9 \text{ megahertz}$$

the effects of the line perturbation can be ignored. Above this frequency, of course, the effects become more pronounced and the overall transmission line model should then include the equivalent tee circuit.

SECTION III

CONSIDERATIONS FOR PERIODICALLY LOADED TRANSMISSION LINES

In the last section, the reflection coefficient for a single equivalent tee network on an infinite transmission line was considered. It was suggested that if the reflection coefficient were sufficiently small, the effects of the network in question could be neglected. This analysis, however, was based on the assumption that the line to the right of the network was infinite and uniform.

As has been noted in ref. (2), aircraft cables often see periodic perturbations along their lengths. Mutual interaction between two adjacent line perturbations can cause a substantial difference in line behavior from the single perturbation case. Hence, lines with periodically spaced discontinuities should be treated with care.

Ref. (8) has investigated the behavior of infinitely long, periodically loaded transmission lines using Floquet's theorem. Various relations for the propagation constant, pass and stop bands, as well as phase and group velocities were developed. The use of the above approach suffers from a number of difficulties, however. In the actual problem, one is interested in finite lines, not infinite ones. Moreover, it is not usually required to determine the line voltage or current at a point on the transmission line, but

rather, at the load end of the line. This cannot be computed using the Floquet theorem approach. In addition, the impact of periodic loading on the behavior of the transient results is not immediately obvious from the infinite line results.

This section investigates the effect of periodic loading on a finite length of transmission line, and compares the results, when possible, to those obtained from Floquet's theorem.

Consider a transmission line of total length L, characteristic impedance Z_c and propagation constant γ. At N points along the transmission line, there are perturbations in the line, and their effects are represented by a series of lumped parameter tee networks, as shown in Figure 13. These line perturbations are assumed to be at distance ℓ apart, and the physical size of the perturbation is assumed to be small compared to ℓ. Due to the periodicity of the line loading, the entire line may be thought of as consisting of N cascaded fundamental sections of line, as shown in Figure 13b, plus a load and source section which are uniform lines of lengths ℓ_L and ℓ_S respectively.

In this manner, the entire line may be represented as shown in Figure 13c, with the condition

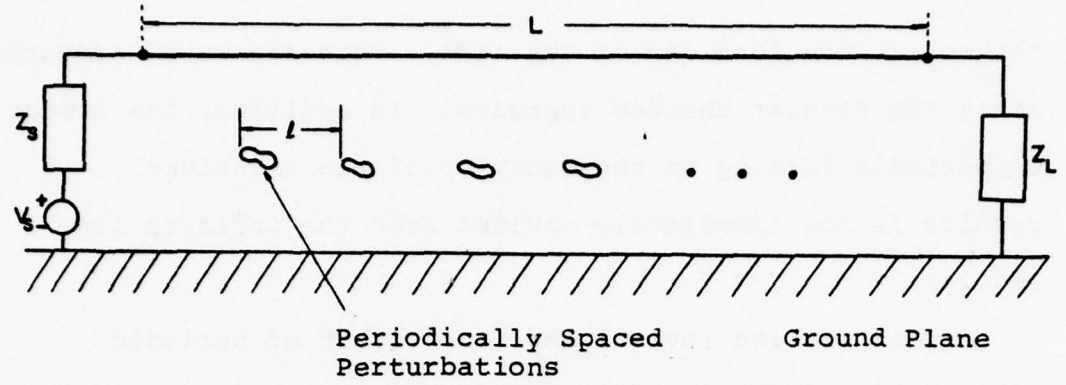

(a)

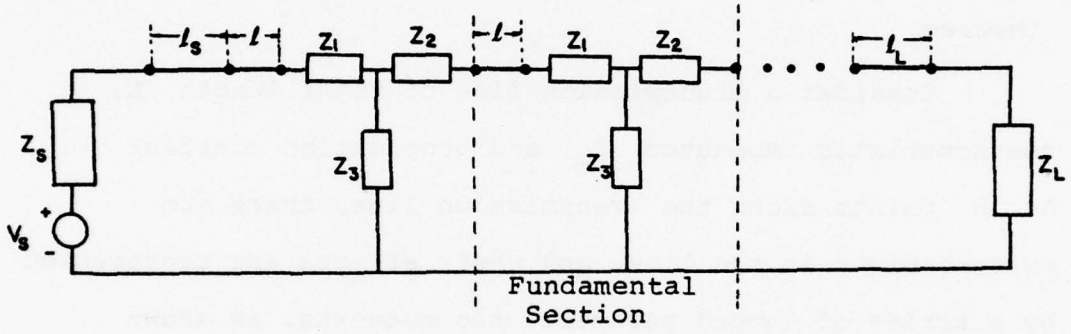

(b)

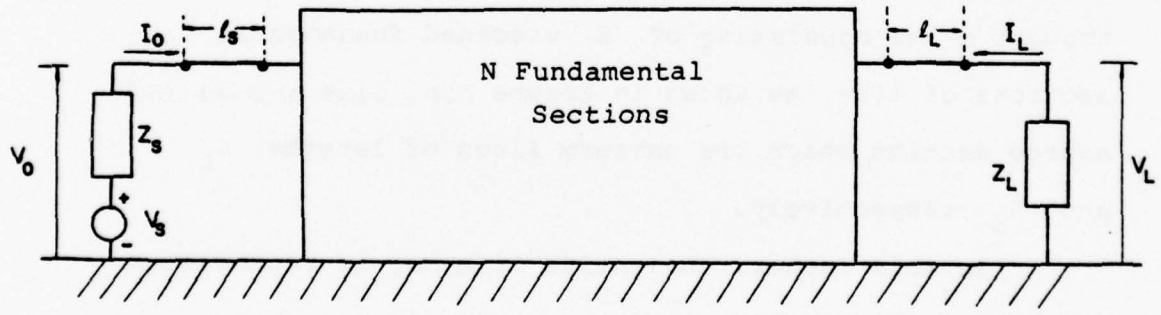

(c)

Figure 13. Geometry of the Finite, Periodically Loaded Transmission Line

$$\ell_S + \ell_L + N\ell = L \tag{18}$$

being enforced.

We are interested in computing the transient voltage induced across the load impedance Z_L. For convenience, we will assume that the source voltage is a step function in time occurring at $t = 0$. To obtain this transient result, we will first obtain a time harmonic expression for the load voltage ($e^{j\omega t}$ time dependence assumed) and later construct the time domain result using Fast Fourier Transform (FFT) methods.

The analysis of a number of transmission lines which are cascaded together (or for that matter, any two-port network) is facilitated by using the chain (or transmission) parameters (ref. 10). Considering a linear two-port network in Figure 14a, the chain parameters A, B, C, D may be used to express V_1 and I_1 in terms of V_2 and I_2 as

$$\begin{bmatrix} V_1 \\ I_1 \end{bmatrix} = \begin{bmatrix} A & B \\ C & D \end{bmatrix} \begin{bmatrix} V_2 \\ -I_2 \end{bmatrix} \tag{19}$$

---

10. Seshu, S., and N. Balabanian, Linear Network Analysis, John Wiley & Sons, New York, 1959.

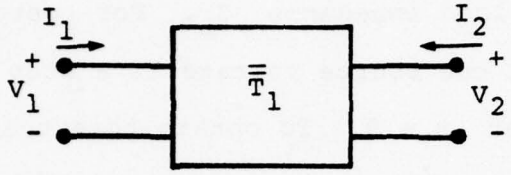

(a)

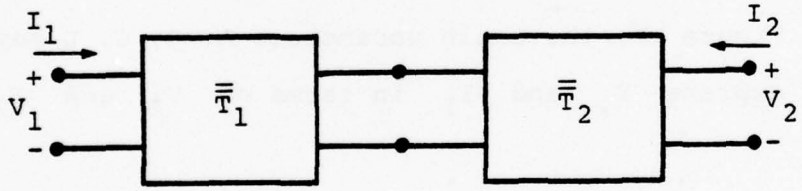

(b)

Figure 14. Voltage and Current Directions of Two-Port Network.

For two networks connected, as in Figure 14b, the V-I relationship is given by the product of two matrices as

$$\begin{bmatrix} V_1 \\ I_1 \end{bmatrix} = \bar{\bar{T}}_1 \cdot \bar{\bar{T}}_2 \begin{bmatrix} V_2 \\ -I_2 \end{bmatrix} \tag{20}$$

where $\bar{\bar{T}}_1$ is the matrix for the first network given by

$$\bar{\bar{T}}_1 = \begin{bmatrix} A_1 & B_1 \\ C_1 & D_1 \end{bmatrix} \tag{21}$$

and $\bar{\bar{T}}_2$ is given by

$$\bar{\bar{T}}_2 = \begin{bmatrix} A_2 & B_2 \\ C_2 & D_2 \end{bmatrix} \tag{22}$$

The fundamental section which comprises the transmission line can be viewed as consisting of two parts, as illustrated in Figure 15. The first is a uniform transmission line of length ℓ and the second is the tee network.

From simple transmission line theory (ref. 11), the transmission matrix for a line of length ℓ is given by

---

11. King, R.W.P., Transmission-Line Theory, Dover, 1965.

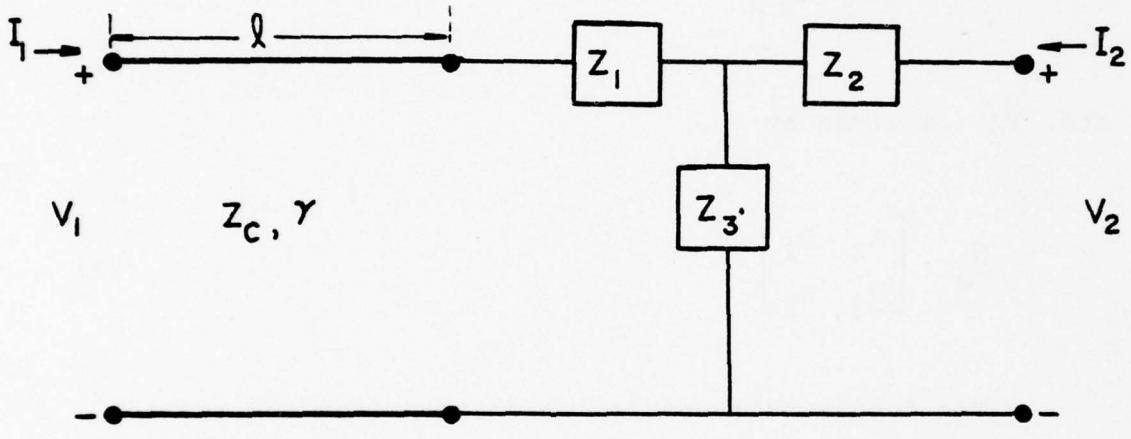

Figure 15. Fundamental Section for Periodic Transmission Line.

$$\bar{\bar{T}}_1 = \begin{bmatrix} \cosh(\gamma \ell) & Z_o \sinh(\gamma \ell) \\ \frac{1}{Z_o} \sinh(\gamma \ell) & \cosh(\gamma \ell) \end{bmatrix} \tag{23}$$

where γ is the propagation constant of the line.

Similarly, simple circuit analysis applied to the equivalent "T" circuit representing the discontinuity gives the following transmission matrix:

$$\bar{\bar{T}}_2 = \begin{bmatrix} 1 + \frac{Z_1}{Z_3} & \frac{1}{Z_3}(Z_1Z_2 + Z_1Z_3 + Z_2Z_3) \\ \frac{1}{Z_3} & 1 + \frac{Z_2}{Z_3} \end{bmatrix} \tag{24}$$

Following Equation (20), the fundamental section of the periodic line can now be described by the transmission matrix, T_S, where

$$\bar{\bar{T}}_S = \bar{\bar{T}}_1 \cdot \bar{\bar{T}}_2$$

which when expanded out, becomes

$$T_S = \begin{Bmatrix} \left[\cosh(\gamma\ell)\left(1+\frac{Z_1}{Z_3}\right)+\frac{Z_o}{Z_3}\sinh(\gamma\ell)\right] & \left[\frac{\cosh(\gamma\ell)}{Z_3}(Z_1Z_2+Z_1Z_3+Z_2Z_3) + Z_o\sinh(\gamma\ell)\left(1+\frac{Z_2}{Z_3}\right)\right] \\ \left[\frac{Z_3+Z_1}{Z_3 Z_o}\sinh(\gamma\ell)+\frac{\cosh(\gamma\ell)}{Z_3}\right] & \left[\frac{\sinh(\gamma\ell)}{Z_3 Z_o}(Z_1Z_2+Z_1Z_3+Z_2Z_3) + \cosh(\gamma\ell)\left(1+\frac{Z_2}{Z_3}\right)\right] \end{Bmatrix} \quad (25)$$

Using this last expression for the transmission through a single fundamental section, the transmission matrix for the entire N section transmission line is given by

$$\bar{\bar{T}}_T = \bar{\bar{T}}_\ell \cdot (\bar{\bar{T}}_S)^N \cdot \bar{\bar{T}}_L \quad (26)$$

where $\bar{\bar{T}}_\ell$ is the transmission line matrix for the line of length ℓ_S and is given by Equation (23) with $\ell = \ell_S$. Similarly, $\bar{\bar{T}}_L$ is the transmission matrix for the line of length ℓ_L. Denoting the individual elements of the total transmission matrix $\bar{\bar{T}}_T$ as A_T, B_T, C_T and D_T, the V-I relationship for the entire line is then given by

$$\begin{bmatrix} V_o \\ I_o \end{bmatrix} = \begin{bmatrix} A_T & B_T \\ C_T & D_T \end{bmatrix} \begin{bmatrix} V_L \\ -I_L \end{bmatrix} \tag{27}$$

At the load, we have the relation that

$$V_L = -Z_L I_L \tag{28}$$

where the minus sign occurs due to our choice of the direction of current flow. Similarly, at the source end of the line, the relationship

$$V_S = V_o + Z_S I_o \tag{29}$$

holds.

Substituting these last two equations into Equation (27), we can solve for the load voltage V_L as

$$V_L = \frac{Z_L V_S}{Z_L A_T + B_T + Z_S (Z_L C_T + D_T)} \tag{30}$$

This expression can be easily evaluated for a large number of frequencies by first performing the chain of matrix multiplications indicated by Equation (26) and then obtaining the parameters A_T, B_T, C_T, and D_T. The time-dependent voltage $v_L(t)$ is then obtained by Fourier inversion.

As an example of the effects of periodic loading on finite transmission lines, a simple tee network model of a cable clamp was used to represent the periodic perturbations on the transmission line. The actual line geometry was that illustrated in Figure 13b, with the lengths ℓ_S and ℓ_L set to zero.

For this example, the series impedance elements Z_1 and Z_2 were chosen to be inductors of 1.0×10^{-9} henrys each, and the shunt impedance element, Z_3, was a capacitor of 9.7×10^{-12} farads. For this case, the unperturbed transmission line characteristic impedance was assumed to be 120 ohms, a value which is consistent with the dimensions of the transmission line passing through the cable clamp. It was assumed that there was a 0.4 meter separation between clamps, so that the fundamental section parameters, as shown in Figure 15, take on the following values:

$$Z_c = 120 \text{ (ohms)}$$

$$\gamma = j\omega/3\times10^{8} \quad (\text{meter}^{-1})$$

$$\ell = .4 \text{ (meter)}$$

$$Z_1 = Z_2 = j\omega\ 1.0\times10^{-9} \text{ (ohms)}$$

$$Z_3 = 1./(j\omega\times9.7\times10^{-12}) \text{ (ohms)}$$

It was assumed that the source and load impedances of the transmission line, Z_S and Z_L, were equal to the line impedance.

Figure 16 shows the magnitude of the load voltage V_L as a function of frequency for various numbers of cable clamps. This represents the delta function spectrum of the load voltage, since the excitation voltage V_S was taken to be unity for all frequencies.

For $N = 0$ (i.e., no cable clamps present), it is seen that the load response is constant in frequency, with a value of 0.5 times the source voltage. As the number of line perturbations increases, it is apparent that distinct pass and stop bands begin to form.

Equations (29) of ref. (8) provides a transcendental equation for the pass and stop band frequencies for the infinite transmission line. These frequency bands are illustrated on Figure 16 for comparison. As may be noted, the pass-stop band structure begins to develop with only two perturbations on the line, and with 10 perturbations, the pass-stop frequencies agree very well with the infinite case.

One difficulty with the infinite line analysis is that there is no information easily obtainable regarding the transient response of the loaded transmission line. Figure 17 shows the computed normalized time domain load voltage for a step-excited source and various numbers of

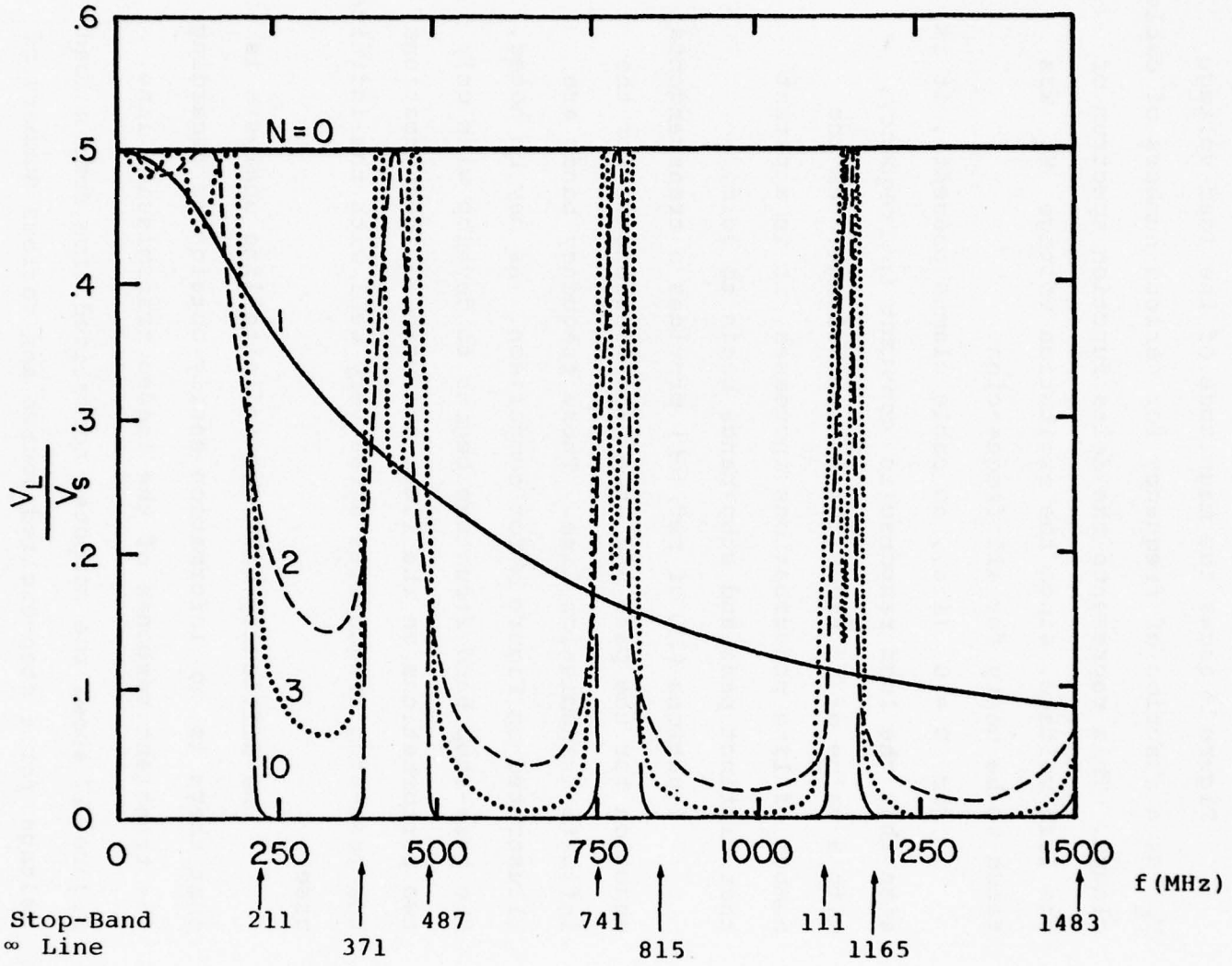

Figure 16. Load voltage magnitude for various numbers of cable clamps.

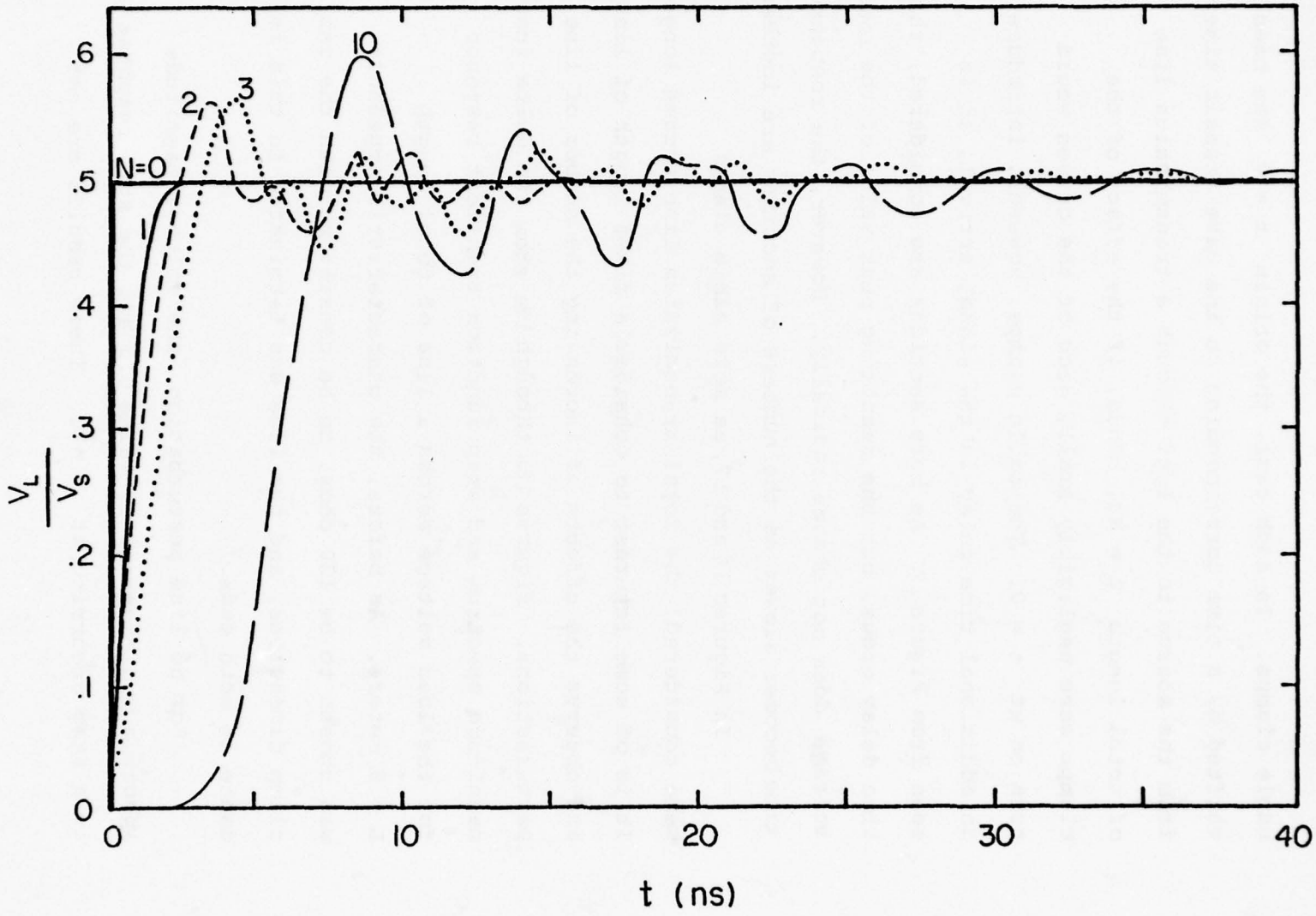

Figure 17. Step function load voltage response for various numbers of cable clamps.

cable clamps. In each case, the origin $t = 0$ has been shifted by a time corresponding to the wave transit time from the source to the load through a transmission line of total length $L = N\ell$. Thus, if the effect of the clamps were negligibly small, each of the curves would turn on at $t = 0$. The cable clamps, however, introduce an additional time delay in the signal arrival, as is seen from Figure 17. As more sections are considered, this time delay grows, but the resulting peak value of the load voltage does not change radically. However, the response rise time becomes slower as the numbers of sections are increased.

In Figures 16 and 17, as more cable clamps were considered, the total transmission line became longer. It is of some interest to consider a fixed length of line and observe the effects of increasing the number of line perturbations. Figures 18a through 18e show the delta function magnitude spectrum and step function transient response for the load voltage across a line of total length $L = 8$ meters. As before, the characteristic impedance was chosen to be 120 ohms, to be consistent with the cable clamp dimensions, and the line was terminated in this impedance at both ends.

For no line perturbation, the voltage magnitude spectrum is a constant of value 0.5 and the step response is a step occurring at $t = 0$. These results are not

presented due to their simplicity. Figure 18a treats the case of a single clamp on the transmission line. The clamp in this case is located at the load end of the line. The effect of this clamp on the load voltage shows up in a high frequency roll-off of the voltage spectrum, and a decrease in the rise time of the transient voltage. For the particular values of impedance elements for the clamp model, it is seen that the effect of the clamp on the load voltage is not particularly significant.

Figures 18b-e show the impluse spectrum and step response of the load voltage for various numbers of identical clamps spaced equally on the transmission line of 8 meters in length. These cases are considerably different from the case of a single clamp, due to the reflection of waves within the various peaks occurring in the transient response, as well as create the pass-stop band structure in the spectrum.

In some circumstances, a set of obstacles near the transmission line may present only a strong capacitive discontinuity to waves propagating on the line. In these cases, we may neglect the inductive elements in the Tee model of the obstacle and treat the line with periodic capacitive loading. Such would be the case of a line passing over a series of thin ribs protruding from the

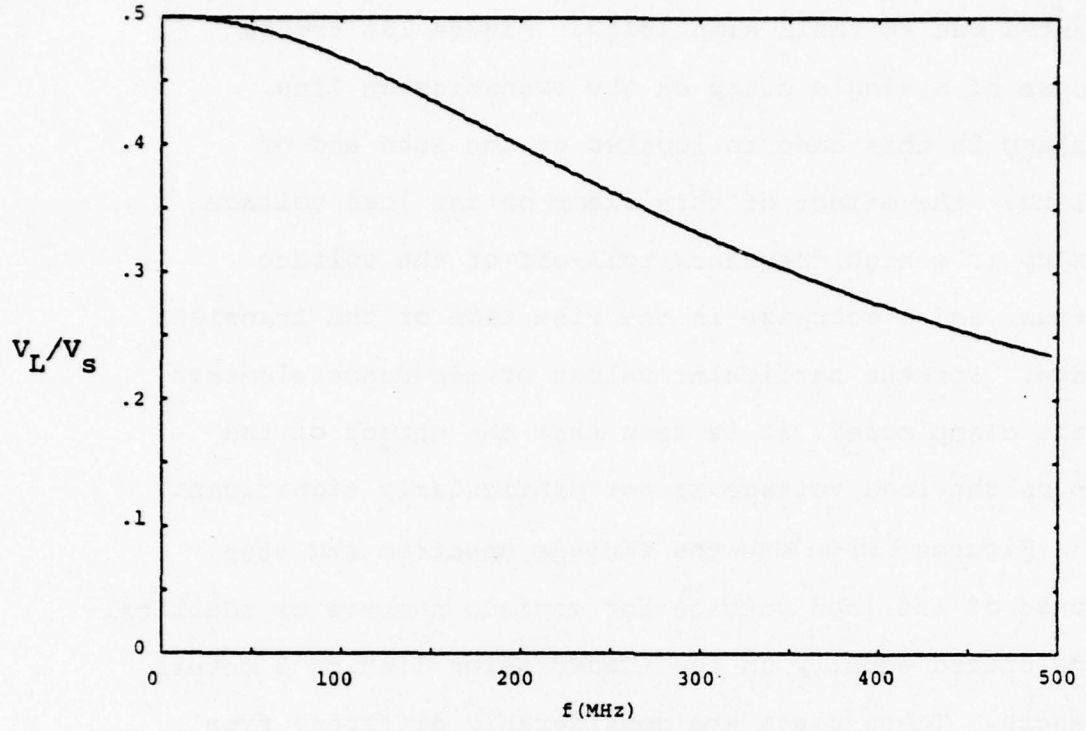

(i)

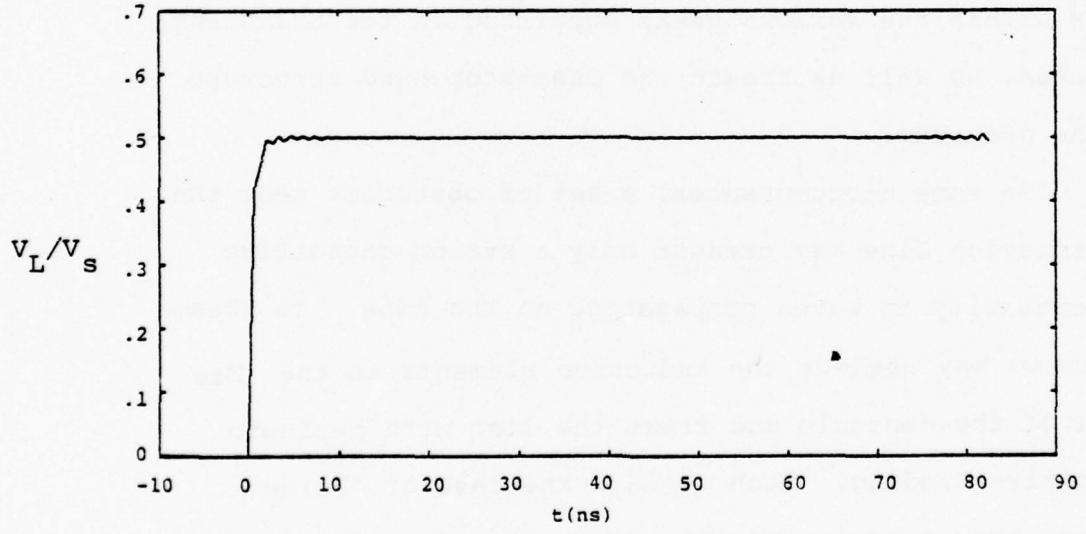

(ii)

Figure 18a. Magnitude of load voltage impulse spectrum (i) and step excited time response (ii) for an 8-meter line with 1 cable clamp.

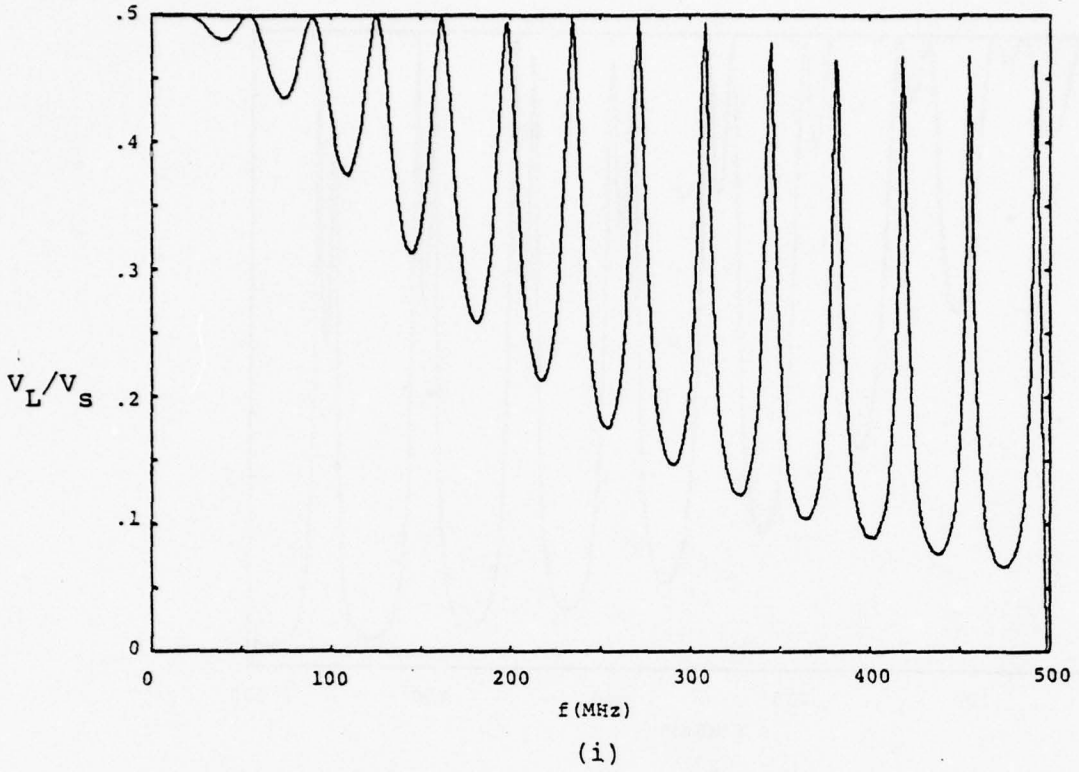

(i)

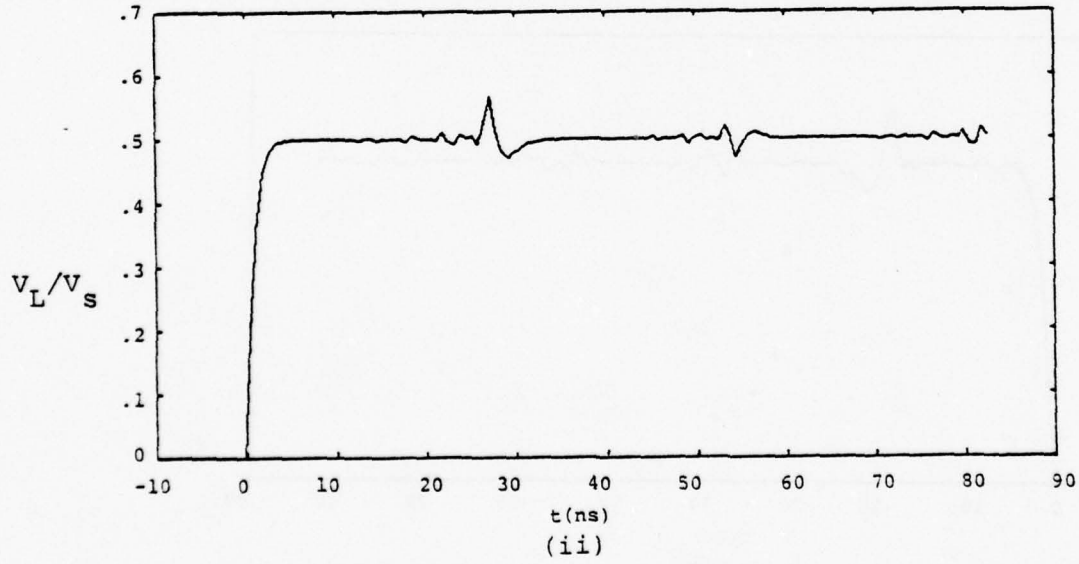

(ii)

Figure 18b. Magnitude of load voltage impulse spectrum (i) and step excited time response (ii) for an 8-meter line with 2 cable clamps.

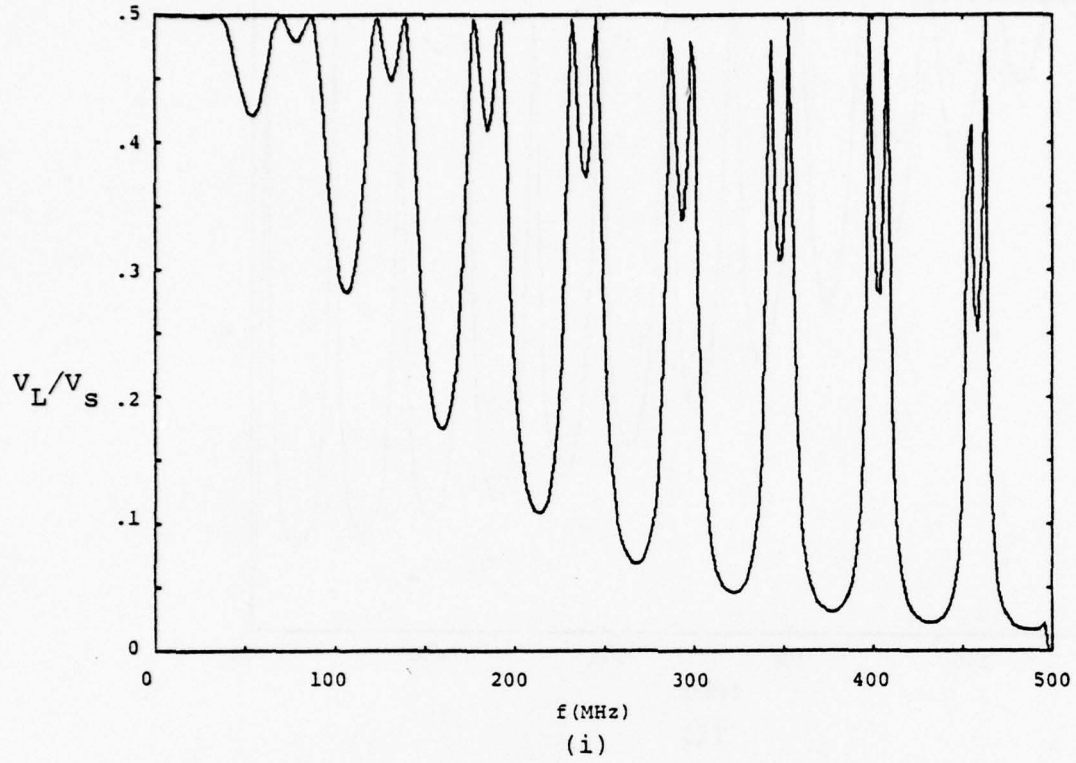

(i)

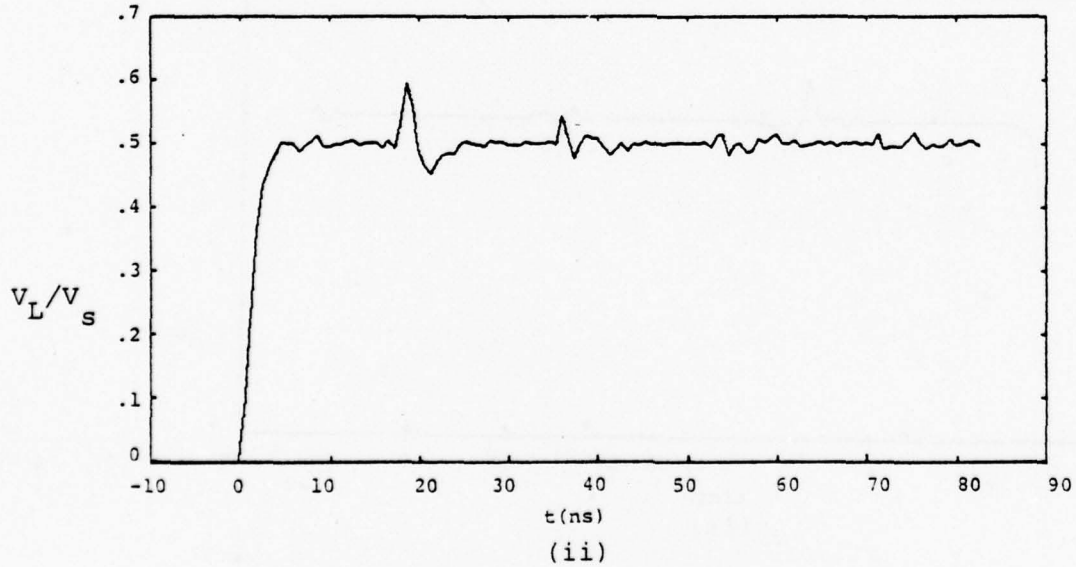

(ii)

Figure 18c. Magnitude of load voltage impulse spectrum (i) and step excited time response (ii) for an 8-meter line with 3 cable clamps.

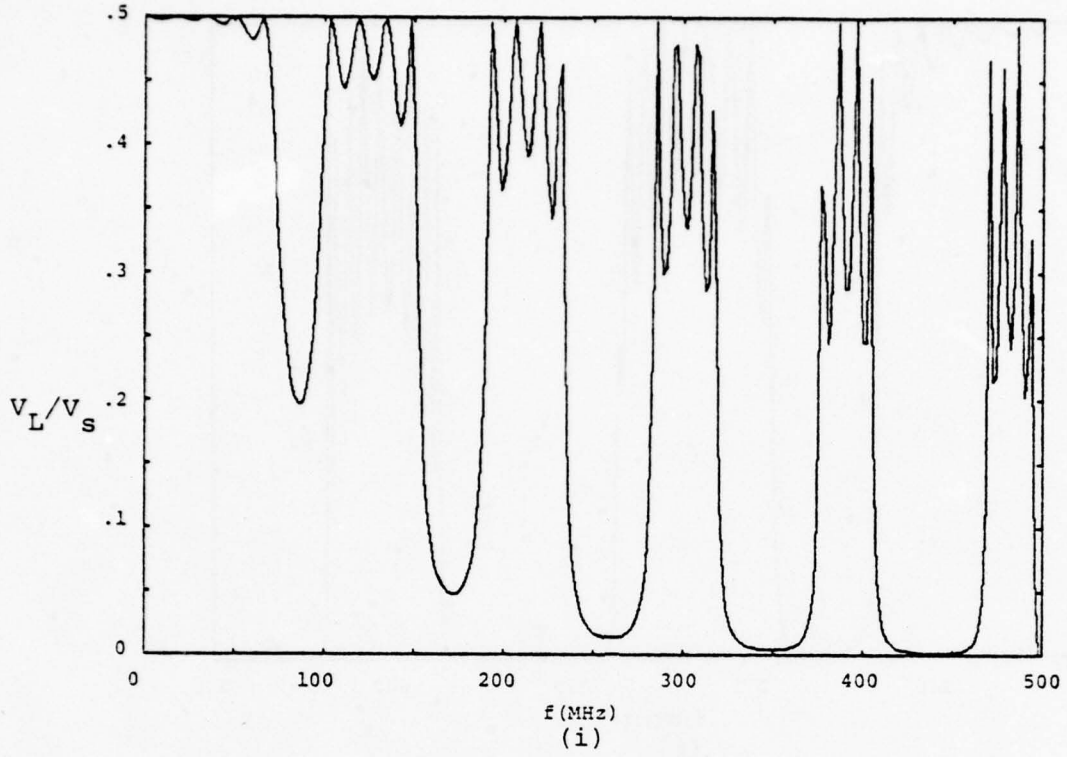

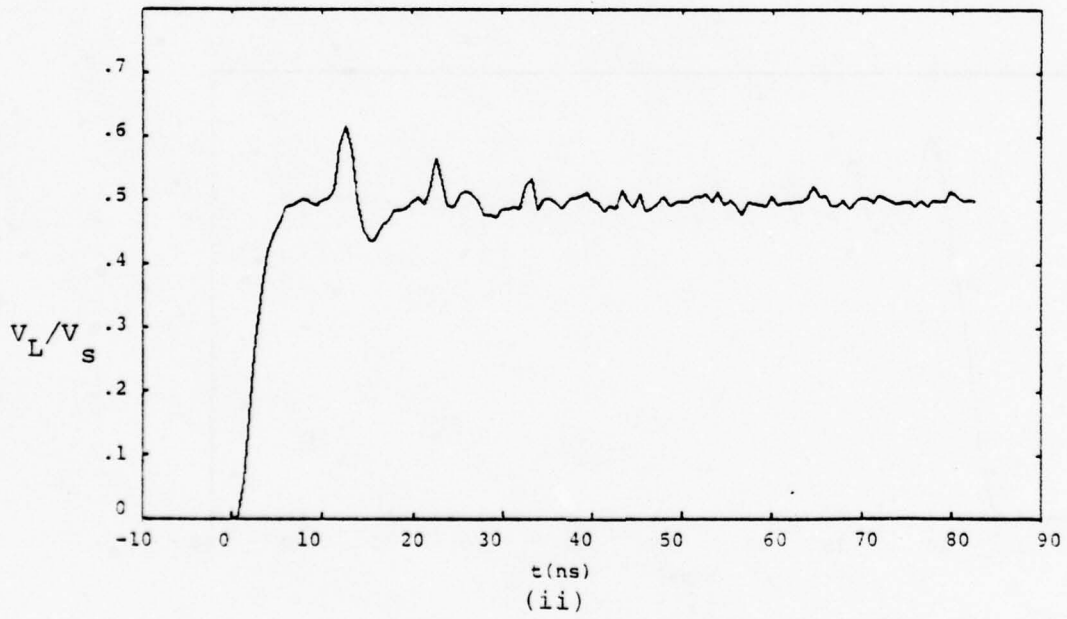

Figure 18d. Magnitude of load voltage impulse spectrum (i) and step excited time response (ii) for an 8-meter line with 5 cable clamps.

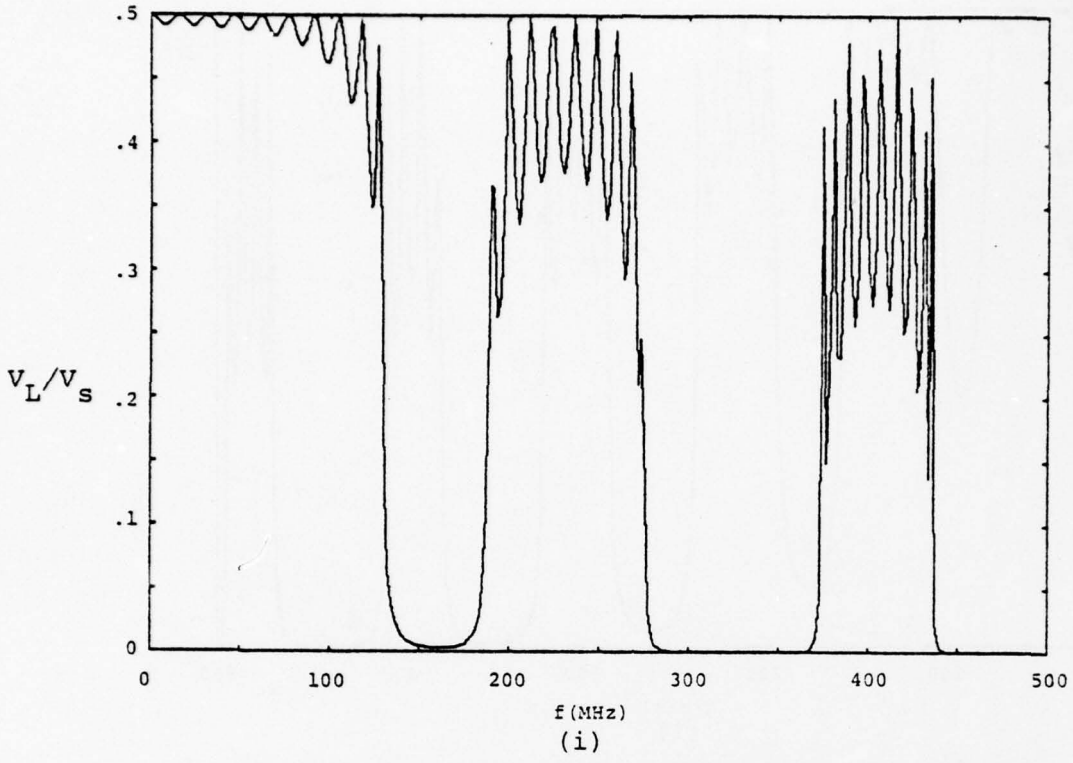

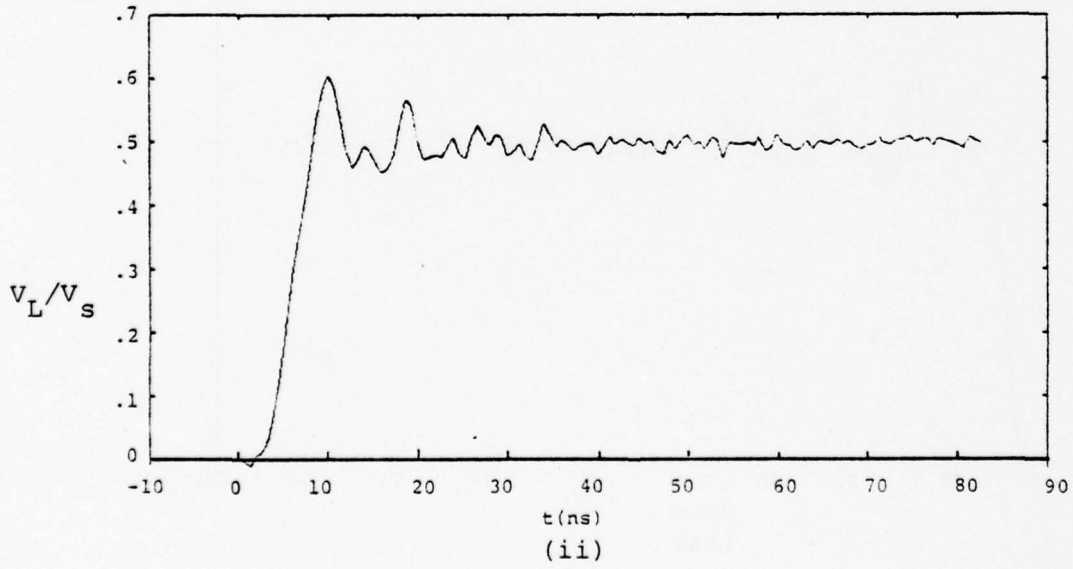

Figure 18e. Magnitude of load voltage impulse spectrum (i) and step excited time response (ii) for an 8-meter line with 10 cable clamps.

ground plane. Figures 19a through 19e show the effects of such periodic capacitance loading on a typical transmission line.

For this example, a transmission line of characteristic impedance $Z_o = 100\,\Omega$ and length $L = 8$ meters was loaded with 10 equally spaced capacitances. The line was matched at both the input and output ends and the load voltage impulse spectrum and step response was computed for various values of capacitive loading. For the transmission line under consideration, the line capacitance per unit length C' was 3.33×10^{-10} farads/meter, thus giving a total capacitance of $C_s = C'\times\ell = 2.66\times10^{-10}$ farads for each section of transmission line between the periodic capacitances. Values of the capacitive loading were $C/C_s = 0.00375$, 0.0375, 0.1, 0.1875, and 0.375, where C represents the capacitance of the rib.

As may be noted in Figure 19, the presence of the capacitance discontinuities has a marked effect on the spectrum of the load voltage. However, for the transient response, the major effect of the periodic loading is in a time delay caused by a slowing of the group velocity on the transmission line. The peak of the transient voltage waveform across the load at times exceeds the voltage predicted without considering the capacitances in the line. This over-voltage, however is seen to be only about 25% of the peak value in the worst case, and may not be

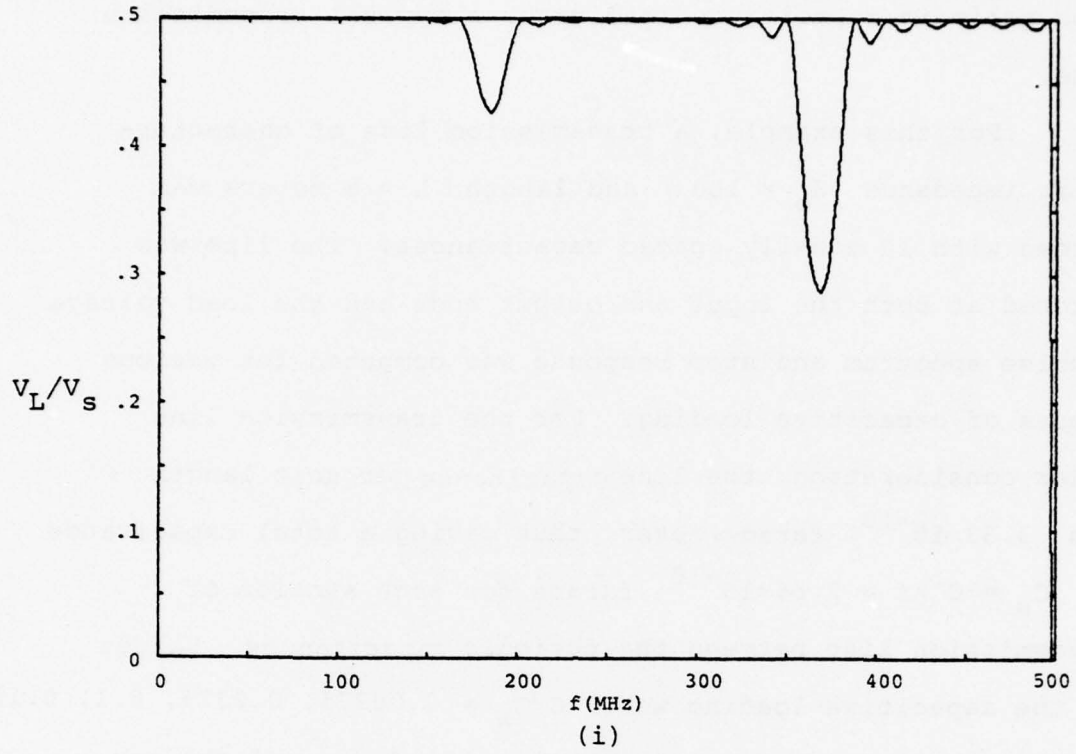

(i)

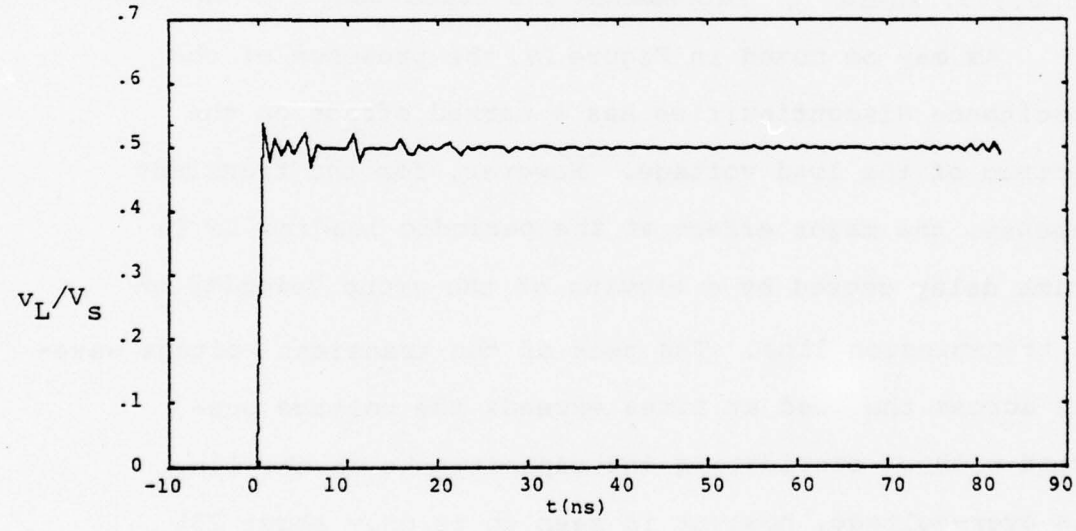

(ii)

Figure 19a. Magnitude of load voltage impulse spectrum (i) and step excited time response (ii) for an 8-meter, 100 ohm, transmission line with 10 capacitive discontinuities of $C/C_s = 0.00375$.

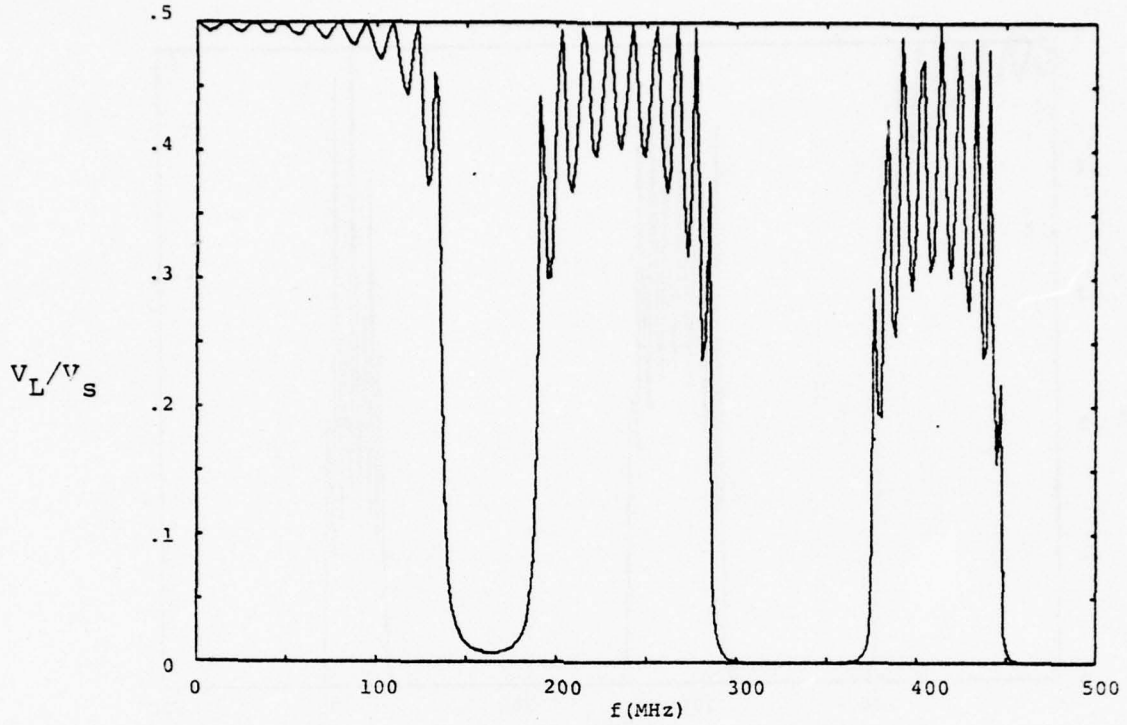

(i)

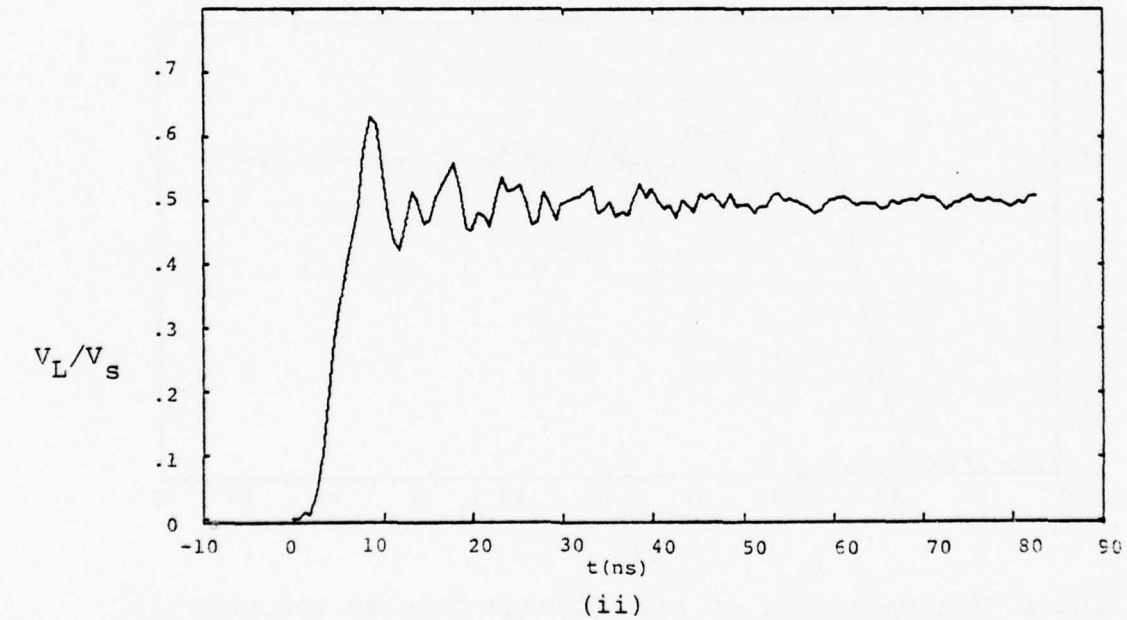

(ii)

Figure 19b. Magnitude of load voltage impulse spectrum (i) and step excited time response (ii) for an 8-meter, 100 ohm, transmission line with 10 capacitive discontinuities of $C/C_s = 0.0375$.

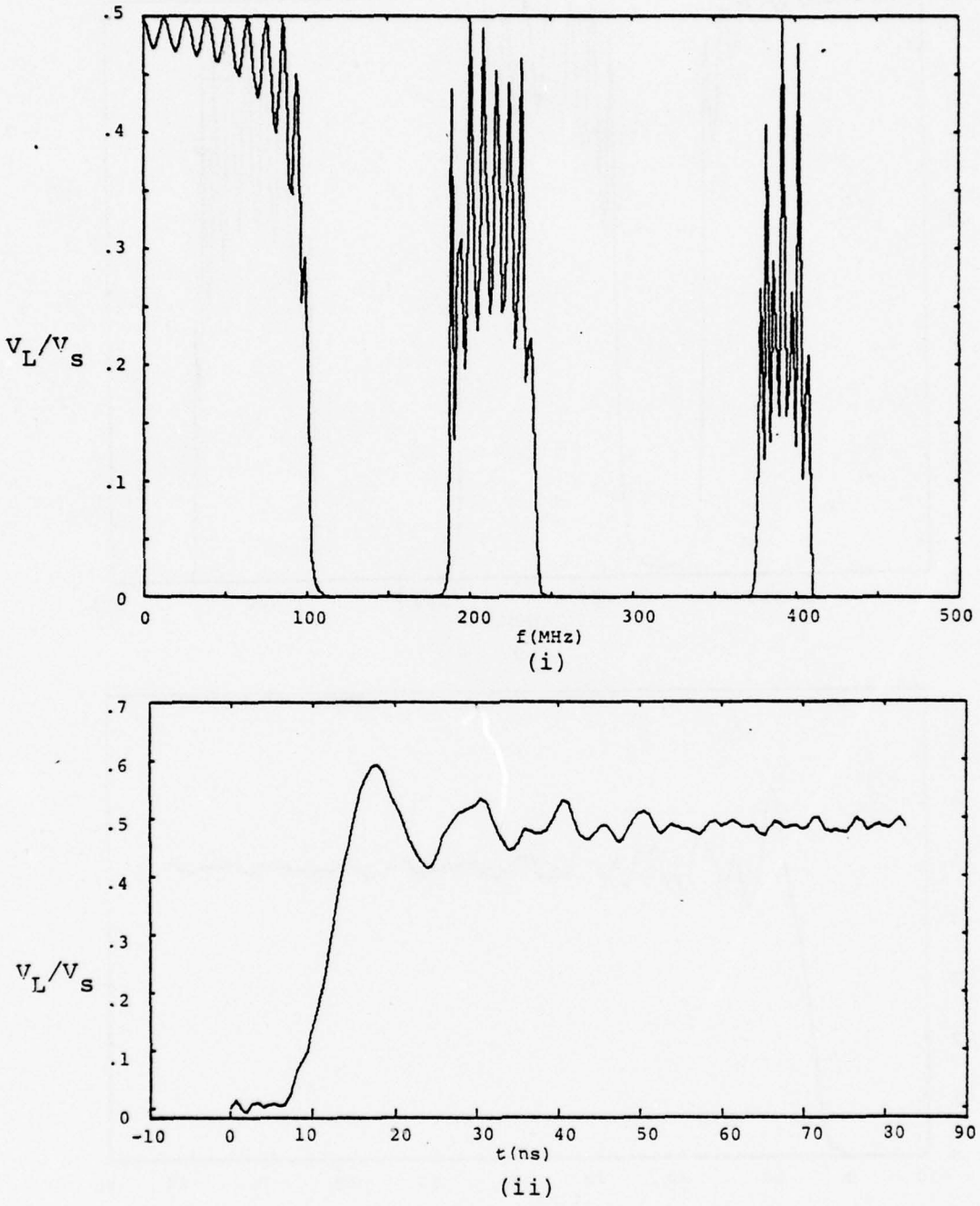

Figure 19c. Magnitude of load voltage impulse spectrum (i) and step excited time response (ii) for an 8-meter, 100 ohm, transmission line with 10 capacitive discontinuities of $C/C_s = 0.1$.

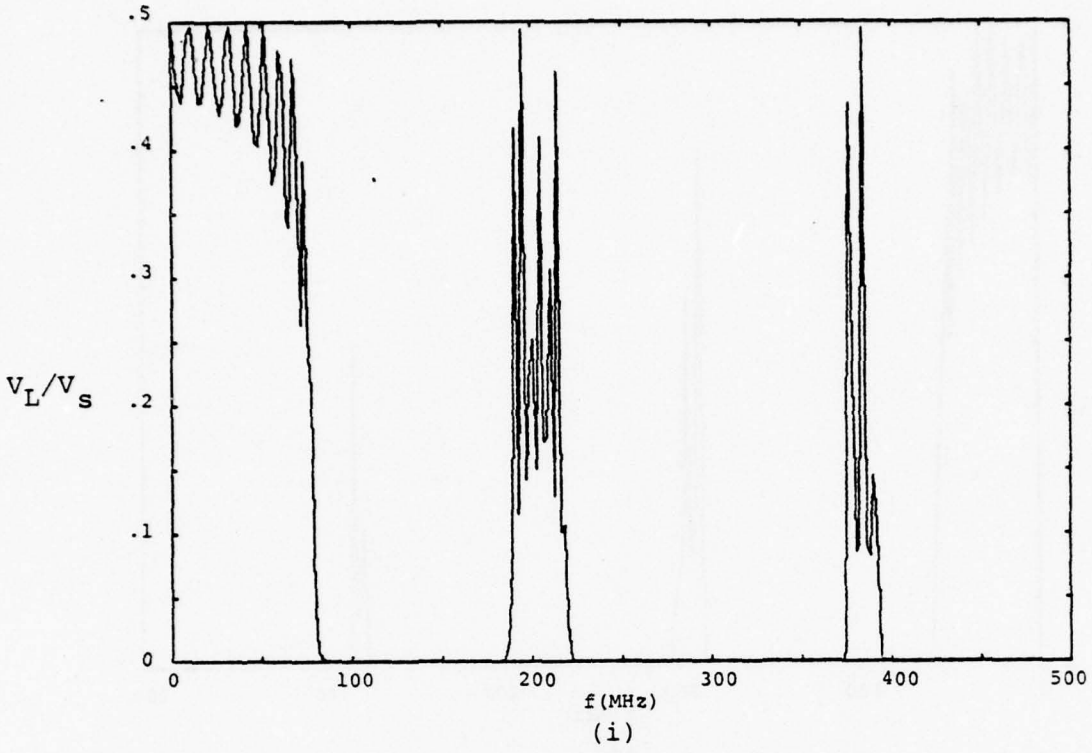

(i)

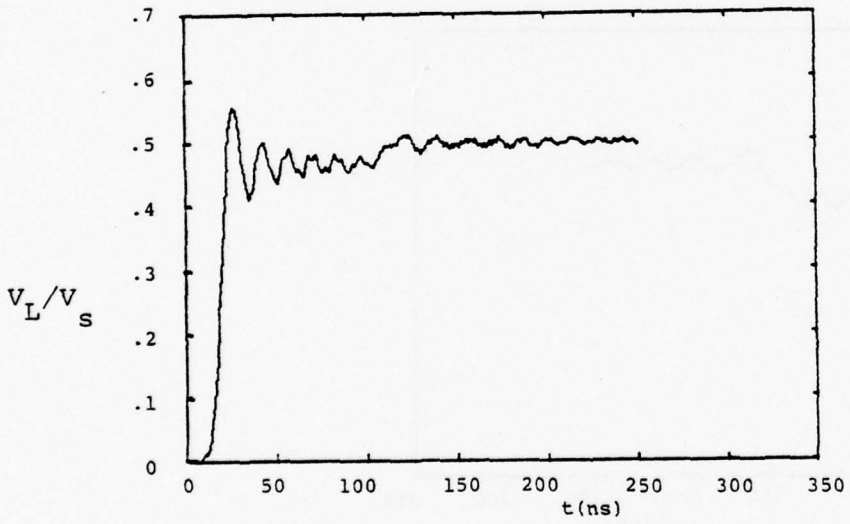

(ii)

Figure 19d. Magnitude of load voltage impulse spectrum (i) and step excited time response (ii) for an 8-meter, 100 ohm, transmission line with 10 capacitive discontinuities of $C/C_s = 0.1875$.

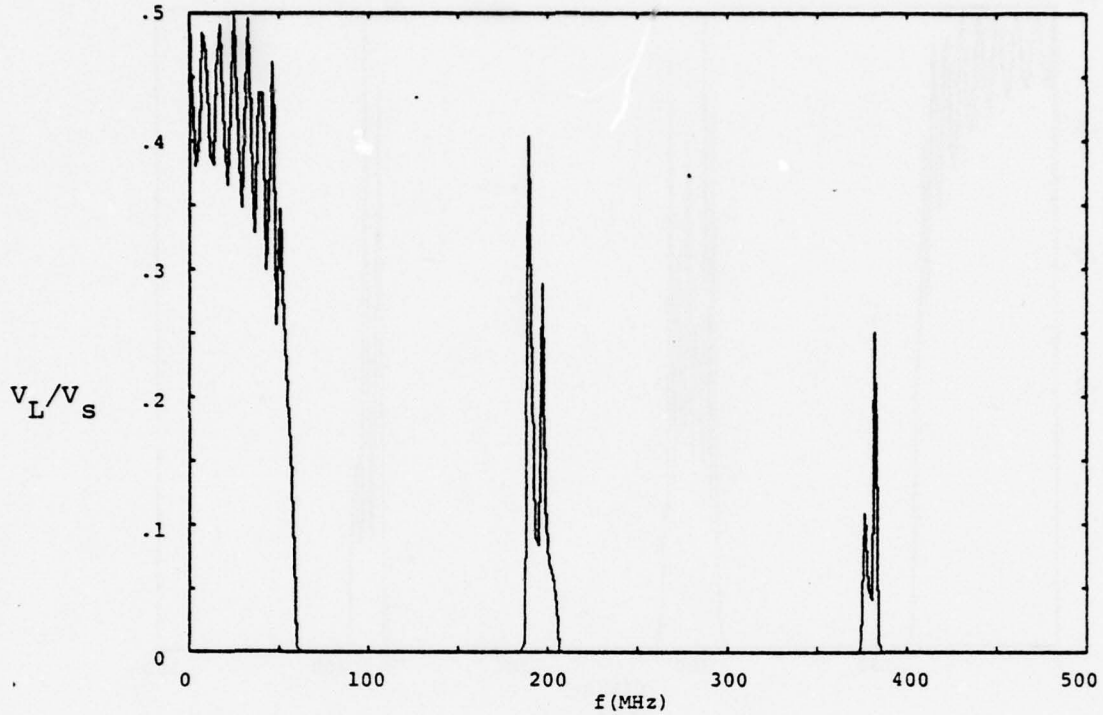

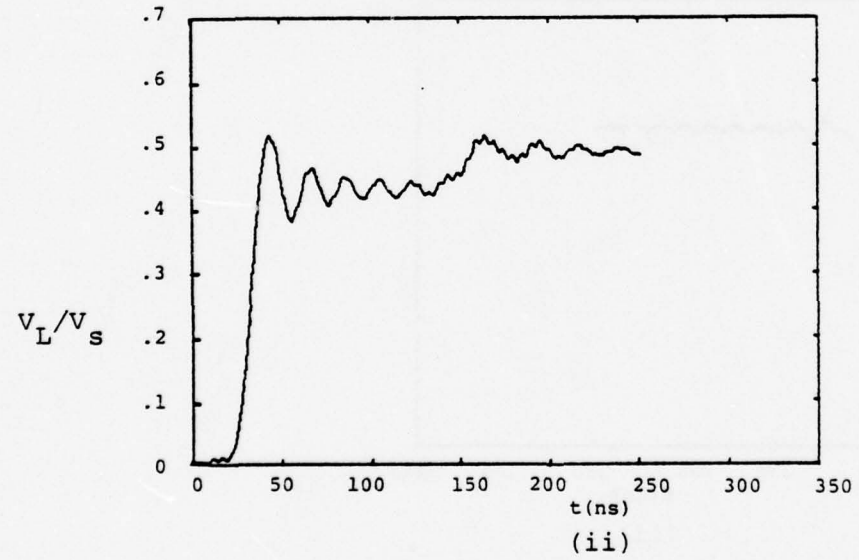

Figure 19e. Magnitude of load voltage impulse spectrum (i) and step excited time response (ii) for an 8-meter, 100 ohm, transmission line with 10 capacitive discontinuities of $C/C_s = 0.375$.

particularly important if only order of magnitude responses are desired. Figure 20 shows the difference between the peak voltage with the capacitance present, and the voltage without capacitance, expressed as a percentage of the latter, as a function of the normalized discontinuity capacitance C/C_s. However, as observed in Figure 19, the rise time of the voltage response increases for larger discontinuity capacitance.

It is difficult to draw many general conclusions from this study of a particular line perturbation other than to say that care should be exercised in defining the electrical model for internal EMP calculations. Periodically spaced obstacles can have a marked effect on transmission line behavior and may be required in a model if accurate results are desired. The techniques discussed here can be easily utilized in a transmission line analysis for treating a specific case.

From an examination of the computed results in the previous figures, it is apparent that there is a much more pronounced effect in the frequency domain response than in the transient results. This is because the step function voltage driving the transmission line has a rather large bandwidth, encompassing many pass and stop bands. The effects of the pass-stop band nature are therefore somewhat masked through the Fourier transform process in going to the time domain.

If one assumes a more realistic voltage waveform, such as a damped sine wave, which would correspond to the excitation provided by skin currents and charges induced on

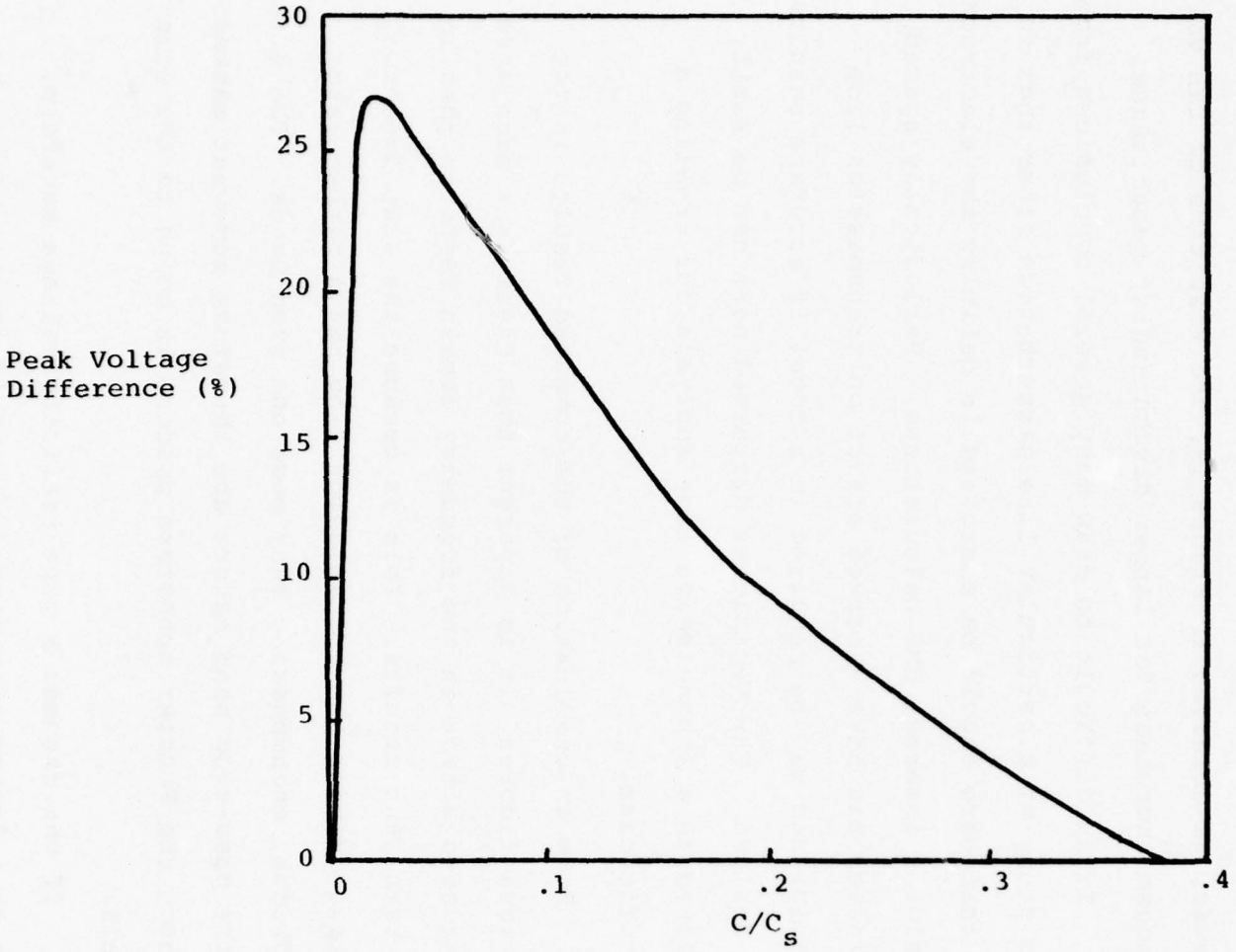

Figure 20. Plot of Difference between Load Voltage with Capacitive Discontinuity and Load Voltage without Discontinuity as a Function of Normalized Capacitance of Discontinuity.

the exterior of an aircraft, it is expected that the pass-stop band nature of the frequency response would be much more important for the transient response. This would be especially true if the fundamental frequency of oscillation of the excitation occurred in the region of a stop band. In that case, very little EMP energy would be transmitted to the load. Such effects must be carefully considered in an EMP system assessment.

SECTION IV

RELATIONSHIPS BETWEEN SINGLE-WIRE TRANSMISSION LINE CURRENT AND THE BULK CURRENT ON A MULTICONDUCTOR LINE

An often used technique for analyzing internal interaction problems is to model multiconductor transmission lines by single wire transmission lines. Not only are the formulation and analysis of problems made simpler, but the computer programs needed to obtain numerical results are relatively simple to write and they execute quickly.

In performing such a simplified analysis, it is desirable to determine the appropriate single line parameters in terms of the parameters defining the multiconductor line. One way to do this is to require that the current on the single wire transmission line have similar behavior to the bulk or total current flowing on a multiconductor line. To assure this requirement, it is necessary to choose an optimum load impedance and characteristic line impedance for the single wire model, using knowledge of the multiconductor line. An alternate way is to equate the single-wire voltage to the averaged quantity of the voltages on the multiconductor line. However, this latter method is not studied here.

Consider an N wire multiconductor transmission line, as shown in Figure 21a. At $z = 0$ there is a generalized termination impedance matrix $\overline{\overline{Z}}_s$ and at $z = \ell$, there is a similar impedance $\overline{\overline{Z}}_\ell$. At an arbitrary position along the line, there are N voltages relative to the reference conductor (the 0^{th} wire) which are represented in vector

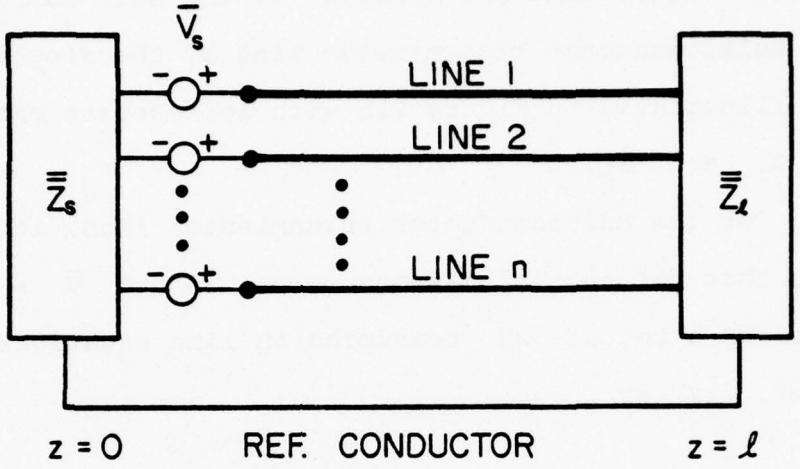

(a)

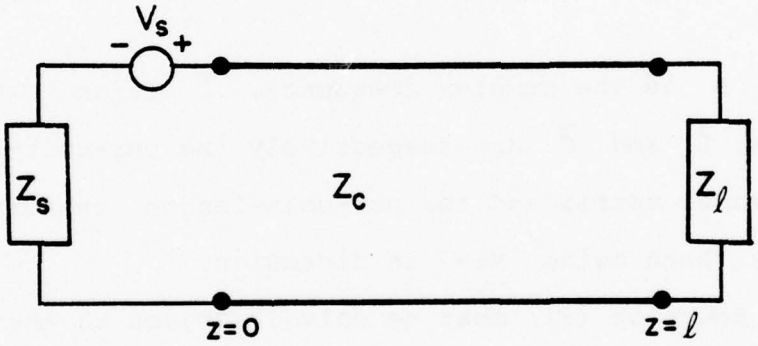

(b)

Figure 21. (a) Voltage Excited Multiconductor Transmission Line and
(b) Equivalent Single Wire Transmission Line

form as $\bar{V}(z)$. Similarly, the wire currents are denoted as $\bar{I}(z)$. Both $\bar{I}$ and $\bar{V}$ are complex N-vectors. It is desired to represent the behavior of the bulk current on this multiconductor transmission line by the single line illustrated in Figure 21b with appropriate choices of Z_s, Z_ℓ and Z_c.

For the multiconductor transmission line, it is well known that the spatial dependence of $\bar{I}$ and $\bar{V}$ are described by a set of 2N transmission line equations given in ref. (12) as

$$\frac{d}{dz}\begin{pmatrix}\bar{V}(z)\\ \bar{I}(z)\end{pmatrix} = -s\begin{pmatrix}\bar{\bar{O}} & \bar{\bar{L}}\\ \bar{\bar{C}} & \bar{\bar{O}}\end{pmatrix}\begin{pmatrix}\bar{V}(z)\\ \bar{I}(z)\end{pmatrix} \tag{31}$$

where s is the complex frequency, $\bar{\bar{O}}$ is an $N\times N$ zero matrix, $\bar{\bar{L}}$ and $\bar{\bar{C}}$ are respectively the per-unit-length inductance matrix and the per-unit-length capacitance matrix, both being $N\times N$ in dimension.

Equation (31) must be solved subject to the appropriate boundary conditions at $z = 0$ and $z = \ell$. For the example of Figure 21, it is seen that these conditions are

---

12. Kajfez, D., "Multi-Conductor Transmission Lines," EMP Interaction Note Series, Note 151, Air Force Weapons Laboratory, Kirtland Air Force Base, NM, June 1972.

$$\bar{V}(0) = \bar{V}_s - \bar{\bar{Z}}_s \bar{I}(0) \qquad (\text{at } z = 0) \tag{32a}$$

and

$$\bar{V}(\ell) = \bar{\bar{Z}}_\ell \bar{I}(\ell) \qquad (\text{at } z = \ell) \tag{32b}$$

Equation (31) can be decoupled to yield two second-order differential equations for $\bar{I}$ and $\bar{V}$ as

$$\frac{d^2\bar{I}}{dz^2} = s^2 \bar{\bar{C}} \bar{\bar{L}} \bar{I}(z) \tag{33}$$

and

$$\frac{d^2\bar{V}}{dz^2} = s^2 \bar{\bar{L}} \bar{\bar{C}} \bar{V}(z) \tag{34}$$

As discussed by Liu (ref. 13), the product $\bar{\bar{C}} \bar{\bar{L}}$ in Equation (33) is often assumed to be a diagonal matrix of the form

$$\bar{\bar{C}} \bar{\bar{L}} = \frac{1}{v^2} \bar{\bar{U}} \tag{35}$$

where $\bar{\bar{U}}$ is the $N \times N$ unity matrix and v is the propagation velocity of waves on the line. This special case occurs for wires in a homogeneous medium.

---

13. Liu, T., "Electromagnetic Coupling between Multiconductor Transmission Lines in a Homogeneous Medium," AFWL-TR-76-333, Air Force Weapons Laboratory, Kirtland Air Force Base, NM, December 1976.

For a multiconductor transmission line in an inhomogeneous dielectric region, such as a bundle of wires each having a dielectric insulation sheath, it is possible to have multiple wave velocities on the transmission line. In that case, moreover, the product $\overline{\overline{C}}\,\overline{\overline{L}}$ is not a simple diagonal matrix as in Equation (35).

As discussed in a series of papers by Paul (refs. 14,15,16), it is possible to diagonalize $\overline{\overline{C}}\,\overline{\overline{L}}$ through the use of a nonsingular $N \times N$ matrix denoted by $\overline{\overline{T}}$, so that

$$\overline{\overline{\gamma}}^2 = s^2\,\overline{\overline{T}}^{-1}\,\overline{\overline{C}}\,\overline{\overline{L}}\,\overline{\overline{T}} \qquad (36)$$

where $\overline{\overline{\gamma}}^2$ is an $n \times n$ diagonal matrix with real positive and nonzero scalars γ_i^2 on the diagonal and zero for the off-diagonal elements.

As discussed by Paul (ref. 14), the matrix $\overline{\overline{T}}$ is easily constructed from the solutions to the eigenvalue equation

---

14. Paul, C.R., "On Uniform Multimode Transmission Lines," IEEE Trans. M.T.T., Vol. MTT-21, No. 8, August 1973, pp. 556-558.

15. Paul, C.R., "Efficient Numerical Computation of the Frequency Response of Cables Illuminated by an Electromagnetic Field," IEEE Trans. M.T.T., Vol. MTT-52, No. 4, April 1974, pp. 454-457.

16. Paul, C.R., "Useful Matrix Chain Parameter Identities for the Analysis of Multiconductor Transmission Lines," IEEE Trans. M.T.T., September 1975, pp. 756-760.

$$\bar{\bar{C}}\,\bar{\bar{L}}\,\bar{\phi}_i = \gamma_i^2\,\bar{\phi}_i \tag{37}$$

where $\bar{\phi}_i$ is the current eigenvector associated with the eigenvalue γ_i^2. The matrix $\bar{\bar{T}}$ is then constructed with various columns being the eigenvector, as

$$\bar{\bar{T}} = (\bar{\phi}_1, \bar{\phi}_2 \ldots \bar{\phi}_N) \tag{38}$$

It is to be noted that the current eigenvectors, $\bar{\phi}_i$, are not functions of position along the line. Physically, these correspond to the distribution of currents on each wire which will propagate together with a propagation constant γ_i.

By introducing a change of variables in the line current as

$$\bar{I}(z) = \bar{\bar{T}}\,\bar{I}_m(z) \tag{39}$$

where $\bar{I}_m(z)$ represents modal currents, the wave equation for the currents becomes

$$\frac{d^2\bar{I}_m(z)}{dz^2} = s^2\,\bar{\bar{T}}^{-1}\,\bar{\bar{C}}\,\bar{\bar{L}}\,\bar{\bar{T}}\,\bar{I}_m \tag{40}$$

or, upon using Equation (36)

$$\frac{d^2\bar{I}_m(z)}{dz^2} = \bar{\bar{\gamma}}^2 \bar{I}_m$$

This equation represents N decoupled scalar equations since the matrix $\bar{\bar{\gamma}}^2$ is diagonalized. The solution to Equation (41) can be written by inspection as

$$\bar{I}_m(z) = e^{-\bar{\bar{\gamma}}z} \bar{\alpha}^+ + e^{\bar{\bar{\gamma}}z} \bar{\alpha}^- \tag{42}$$

where $\bar{\alpha}^+$ and $\bar{\alpha}^-$ represent the magnitudes of forward and backward propagating modes and the term $e^{\bar{\bar{\gamma}}z}$ is a N×N diagonal matrix with elements $e^{\bar{\bar{\gamma}}z}_{i,i} = e^{\gamma_i z}$ and $e^{\gamma z}_{i,j} = 0$ for i, j=1,...N and i≠j.

From Equations (39) and (42), the line current can be expressed directly as

$$\bar{I}(z) = \bar{\bar{T}} (e^{-\bar{\bar{\gamma}}z} \bar{\alpha}^+ + e^{\bar{\bar{\gamma}}z} \bar{\alpha}^-) \tag{43}$$

This last equation can be regarded as the superposition of two traveling waves, as

$$\bar{I}(z) = \bar{I}^+(z) + \bar{I}^-(z) \tag{44}$$

where the superscripts + and - indicate the propagation direction in z.

The voltage on the line can now be found from a portion of Equation (31) as

$$\frac{d\bar{I}(z)}{dz} = -s\,\bar{\bar{C}}\,\bar{V}(z) \tag{45}$$

Using Equation (43) we obtain

$$\bar{V}(z) = \bar{\bar{C}}^{-1}\,\bar{\bar{T}}\,\frac{\bar{\bar{\gamma}}}{s}\,\bar{\bar{T}}^{-1}\left[\bar{\bar{T}}(e^{-\bar{\bar{\gamma}}z}\,\bar{\alpha}^{+} - e^{\bar{\bar{\gamma}}z}\,\bar{\alpha}^{-})\right] \tag{46}$$

and upon defining a characteristic impedance matrix $\bar{\bar{Z}}_c$ as

$$\bar{\bar{Z}}_c = \bar{\bar{C}}^{-1}\,\bar{\bar{T}}\,\frac{\bar{\bar{\gamma}}}{s}\,\bar{\bar{T}}^{-1} \tag{47}$$

the line voltage becomes

$$\bar{V}(z) = \bar{\bar{Z}}_c\,\bar{\bar{T}}(e^{-\bar{\bar{\gamma}}z}\,\bar{\alpha}^{+} - e^{\bar{\bar{\gamma}}z}\,\bar{\alpha}^{-}) \tag{48}$$

or, in terms of forward and backward traveling voltage waves,

$$\bar{V}(z) = \bar{V}^{+}(z) + \bar{V}^{-}(z) \tag{49}$$

In comparing Equations (43) and (48), it is noted that the well-known relationship between the forward and backward propagating line voltage and current waves exists:

$$\bar{V}^{+}(z) = \bar{\bar{Z}}_c \, \bar{I}^{+}(z) \tag{50a}$$

$$\bar{V}^{-}(z) = -\bar{\bar{Z}}_c \, \bar{I}^{-}(z) \tag{50b}$$

The unknown modal coefficients $\bar{\alpha}^{+}$ and $\bar{\alpha}^{-}$ must be determined through the use of the boundary conditions of Equations (32a) and (32b).

By defining modal current reflection matrices, $\bar{\bar{\rho}}$, as

$$\bar{\bar{\rho}}_s = \bar{\bar{T}}^{-1} \, (\bar{\bar{Z}}_s + \bar{\bar{Z}}_c)^{-1} \, (\bar{\bar{Z}}_s - \bar{\bar{Z}}_c) \, \bar{\bar{T}} \qquad (\text{at } z = 0) \tag{51}$$

and

$$\bar{\bar{\rho}}_\ell = \bar{\bar{T}}^{-1} \, (\bar{\bar{Z}}_\ell + \bar{\bar{Z}}_c)^{-1} \, (\bar{\bar{Z}}_\ell - \bar{\bar{Z}}_c) \, \bar{\bar{T}} \qquad (\text{at } z = \ell) \tag{52}$$

solutions for $\bar{\alpha}^{+}$ and $\bar{\alpha}^{-}$ can be obtained and substituted into Equation (43) to yield the following expression for the current on the multiconductor line

$$\bar{I}(z) = \bar{\bar{T}}(e^{-\bar{\bar{\gamma}}z} - e^{\bar{\bar{\gamma}}(z-\ell)} \, \bar{\bar{\rho}}_\ell \, e^{-\bar{\bar{\gamma}}\ell})(\bar{\bar{U}} - \bar{\bar{\rho}}_s \, e^{-\bar{\bar{\gamma}}\ell} \, \bar{\bar{\rho}}_\ell \, e^{-\bar{\bar{\gamma}}\ell})^{-1}$$

$$\times \bar{\bar{T}}^{-1} \, (\bar{\bar{Z}}_c + \bar{\bar{Z}}_s)^{-1} \, \bar{V}_s \tag{53}$$

The reflection matrix, $\bar{\bar{\rho}}$, provides information on how a particular mode, say the i^{th} mode, reflects and excites other modes which propagate away from the load.

For example, the element $\overline{\overline{\rho}}_{i,i}$ is the self-reflection coefficient for the i^{th} mode, and $\overline{\overline{\rho}}_{i,j}$ is the coefficient for determining the strength of the j^{th} reflected mode due to the i^{th} incident mode.

As can be seen from Equation (52), if the multiconductor line is matched (i.e., $\overline{\overline{Z}}_s = \overline{\overline{Z}}_\ell = \overline{\overline{Z}}_c$), the reflection matrix is a zero matrix. Under this assumption, the relation for the transmission line current from Equation (53) simplifies considerably to yield

$$\overline{I}(z) = \overline{\overline{T}}\, e^{-\overline{\overline{\gamma}}z}\, \overline{\overline{T}}^{-1}\, (2\overline{\overline{Z}}_c)^{-1}\, \overline{V}_s \tag{54}$$

For most EMP analysis problems, however, it is not possible to assume a perfectly matched multiconductor line because, as discussed in ref. (17), matched impedance load consists not only of impedance elements from each wire to ground (the diagonal terms in $\overline{\overline{Z}}_L$) but also of impedances between the various wires (the off diagonal terms in $\overline{\overline{Z}}_L$).

The total or "bulk" current on the multiconductor transmission line can be obtained by adding all of the individual wire currents found from Equation (53) as

$$I_B(z) = \sum_{i=1}^{N} I(z)_i \tag{55}$$

---

17. Frankel, S., Cable and Multi-Conductor Transmission Analysis, Harry Diamond Laboratories, HDL-TR-091-1, June 1974.

Here, $I(z)_i$ represents the i^{th} element of the line current vector $\bar{I}(z)$. As may be noted from Equation (53), this is a very complicated function of the terminating impedances $\bar{\bar{Z}}_s$ and $\bar{\bar{Z}}_\ell$.

A similar scalar analysis of the transmission line of Figure 21b leads to the following equation for the single line current:

$$I(z) = \frac{e^{-\gamma z} - \rho_\ell \, e^{\gamma(z-2\ell)}}{1 - \rho_\ell \, \rho_s \, e^{-2\gamma\ell}} \frac{V_s}{Z_c + Z_s} \tag{56}$$

where

$$\rho_\ell = \frac{Z_\ell - Z_c}{Z_\ell + Z_c} \tag{57}$$

and

$$\rho_s = \frac{Z_s - Z_c}{Z_s + Z_c} \tag{58}$$

As may be noted, this is simply the scalar version of Equation (53).

The best choice of the single line loads Z_s and Z_ℓ so that the current $I(z)$ approximates $I_B(z)$ is not at all obvious. It is possible, however, to make a few simplifications of Equation (53) to gain insight into the modal nature of the multiconductor current.

A close examination of the current eigenmodes $\bar{\Phi}_i$ of typical multiconductor cables (i.e., the columns of the $\bar{\bar{T}}$ matrix) shows that there is generally one mode of the system which is predominately a bulk mode and the rest of the modes are predominately differential. Thus, in the use of Equation (55) to define the bulk current, it is often found that only one column of $\bar{\bar{T}}$ contributes significantly to the bulk current.

It is often convenient to make the assumption that all modes propagate with the same velocity. Recent studies (ref. 18) indicate that the effects of multivelocity modes are not extremely important in determining the transient response of a load for a step waveform. For others, it may be important. This assumption is expressed in Equation (35) and implies that the eigenvalues of the matrix $\bar{\bar{C}}\,\bar{\bar{L}}$ are all the same. Thus, the exponential matrix $e^{-\bar{\bar{\gamma}}z}$ in Equation (53) becomes $e^{-\gamma z}\,\bar{\bar{U}}$ and the line current may be simplified somewhat as

$$\bar{I}(z) = \bar{\bar{T}}(e^{-\gamma z}\,\bar{\bar{U}} - e^{\gamma(z-2\ell)}\,\bar{\bar{\rho}}_L)(\bar{\bar{U}} - e^{-2\gamma\ell}\,\bar{\bar{\rho}}_s\,\bar{\bar{\rho}}_L)^{-1}$$

$$\times\, \bar{\bar{T}}^{-1}(\bar{\bar{Z}}_c + \bar{\bar{Z}}_s)^{-1}\,\bar{V}_s \qquad (59)$$

---

18. C.E. Baum, T.K. Liu, F.M. Tesche and S.K. Chang, "Numerical Results for Multiconductor Transmission-Line Networks," AFWL-TR-77-123, Air Force Weapons Laboratory, Kirtland Air Force Base, NM, June 1977.

Since the eigenvalues of $\bar{\bar{C}}\,\bar{\bar{L}}$ are identical for this case, there is considerable freedom in choosing the transformation matrix $\bar{\bar{T}}$. The main requirement is, of course, that the eigenvectors of $\bar{\bar{C}}\,\bar{\bar{L}}$ be linearly independent. One particularly common choice for $\bar{\bar{T}}$ is the identity matrix, $\bar{\bar{U}}$. This implies that for the i^{th} mode, there is a unit current on the i^{th} wire with zero currents on all others.

With this choice of $\bar{\bar{T}}$, Equation (59) for the line current reduces to

$$\bar{I}(z) = (e^{-\gamma z}\,\bar{\bar{U}} - e^{\gamma(z-2\ell)}\,\bar{\bar{\rho}}_L)(\bar{\bar{U}} - e^{-2\gamma\ell}\,\bar{\bar{\rho}}_s\,\bar{\bar{\rho}}_L)^{-1}(\bar{\bar{Z}}_c + \bar{\bar{Z}}_s)^{-1}\,\bar{V}_s \tag{60}$$

which is the same as Equation (8) of ref. (13). Because each mode contributes to the total or bulk current, it is necessary to employ Equation (55) to calculate I_B.

It is possible, however, to simplify the analysis somewhat by choosing a different form of $\bar{\bar{T}}$. Consider a transformation matrix of the form

$$T = \begin{bmatrix} 1 & -1 & -1 \ldots -1 & -1 \\ 1 & 1 & 0 \ldots 0 & 0 \\ 1 & 0 & 1 \ldots 0 & 0 \\ \vdots & \vdots & \vdots \ddots \vdots & \vdots \\ 1 & 0 & 0 \ldots 1 & 0 \\ 1 & 0 & 0 \ldots 0 & 1 \end{bmatrix} \tag{61}$$

Note that the first mode (the first column of $\bar{\bar{T}}$) is a pure bulk mode, and the other modes give no contribution to the bulk current. It may be easily demonstrated that these modes are linearly independent, and thus will correctly represent the current flowing on the multiconductor line.

From Equation (59), it is possible to identify various mechanisms which excite the different modes on the transmission line. The first, and most obvious, is the source term $\bar{V}_s$. As shown in Figure 21a, $\bar{V}_s$ represents n voltage sources at one end of the transmission line.

One could, by a clever choice of the elements of $\bar{V}_s$, determine an excitation which excites only the bulk mode. This would be the $\bar{V}_s$ which satisfies the equation

$$\bar{\bar{T}}^{-1}(\bar{\bar{Z}}_c + \bar{\bar{Z}}_s)^{-1}\,\bar{V}_s = \alpha \begin{bmatrix} 1 \\ 0 \\ 0 \\ \vdots \\ \cdot \end{bmatrix} \tag{62}$$

where α is an arbirary constant. Solving for $\bar{V}_s$, we find

$$\bar{V}_s = \alpha(\bar{\bar{Z}}_c + \bar{\bar{Z}}_s)\,\bar{\bar{T}} \begin{bmatrix} 1 \\ 0 \\ 0 \\ \vdots \\ \cdot \end{bmatrix} \tag{63}$$

and upon performing the multiplication of the $\bar{\bar{T}}$ matrix given in Equation (61) and the vector $\begin{bmatrix} 1 \\ 0 \\ 0 \\ \vdots \end{bmatrix}$,

$\bar{V}_s$ may be expressed as

$$\bar{V}_s = \alpha (\bar{\bar{Z}}_c + \bar{\bar{Z}}_s) \begin{bmatrix} 1 \\ 1 \\ 1 \\ \vdots \end{bmatrix} \tag{64}$$

or, equivalently, in component form as

$$\bar{V}_{s_i} = \alpha \sum_{j=1}^{N} \bar{\bar{Z}}_{c_{i,j}} + \bar{\bar{Z}}_{s_{i,j}} \tag{65}$$

Thus, when the N wire voltage sources satisfy Equation (65), only the bulk mode will be excited. For a realistic cable, however, there is no way to assure that the excitation will be of this type. It should be noted in passing that a similar development can be carried out for current sources exciting the multiconductor line. An incident electromagnetic field on the transmission line will induce both voltage and current sources along the line and, hence, both types of sources must be considered.

A second mechanism for the excitation of the various modes is through the reflection coefficient matrices, $\bar{\bar{\rho}}_\ell$ and $\bar{\bar{\rho}}_s$. As has been discussed, the i,j^{th} element of $\bar{\bar{\rho}}$ indicates the magnitude of the j^{th} reflected mode excited by the i^{th} mode incident on a load. With the choice of $\bar{\bar{T}}$ in Equation (61), the first row of the $\bar{\bar{\rho}}$ matrix indicates the excitation of other differential modes due to the bulk mode incident on the load.

If $\overline{\overline{\rho}}$ is a diagonal matrix, then there is no mode conversion at the load. An incident bulk mode would be reflected as a bulk mode. If the excitation were purely bulk in nature, as excited by the voltage of Equation (65), then only a bulk wave would exist on the line. In examining Equation (52), it is evident that $\overline{\overline{\rho}}_\ell$ will be a diagonal matrix if the matrix $(\overline{\overline{Z}}_\ell + \overline{\overline{Z}}_c)^{-1}\ (\overline{\overline{Z}}_\ell - \overline{\overline{Z}}_c)$ is the identity matrix. This will happen if $\overline{\overline{Z}}_\ell$ equals zero (all lines shorted together and grounded). Generally, however, it is to be expected that the reflection coefficient is not a diagonal matrix.

There is one interesting case where $\overline{\overline{\rho}}$ is diagonal, due to assumed symmetries in the characteristic impedance matrix. Suppose that a multiconductor cable consists of N <u>identical</u> wires which are randomly positioned within the cable (ref. 19). If the cable length is sufficiently long compared with the distance over which the wires' positions change in the cable, it is possible to then define the capacitive coefficient matrix using only two numbers: 1) an average capacitance coefficient along the diagonal, and 2) an average of the off-diagonal terms.

---

19. Morgan, M.A., and F.M. Tesche,"Statistical Analysis of Critical Load Excitations Induced on a Random Cable System by an Incident Driving Field: Basic Concepts and Methodology," AFWL-TR-75-281, Air Force Weapons Laboratory, Kirtland Air Force Base, NM, July 1975.

With the assumption of a single propagation velocity, the above conditions lead to a characteristic impedance matrix which has the elements $\bar{\bar{Z}}_{c_{i,i}} = Z_1$, $\bar{\bar{Z}}_{c_{i,j}} = Z_2$ where Z_1 and Z_2 are the two complex impedances which describe this randomly laid line. If the load impedance matrix is also diagonal with all impedances the same, then the matrix $(\bar{\bar{Z}}_\ell + \bar{\bar{Z}}_c)^{-1} (\bar{\bar{Z}}_\ell - \bar{\bar{Z}}_c)$ also has a diagonally symmetric form, with all diagonal terms the same, and all off-diagonal terms equal. The multiplication of this resulting matrix by $\bar{\bar{T}}$ and $\bar{\bar{T}}^{-1}$, as in Equation (52), then yields a diagonal matrix for $\bar{\bar{\rho}}$.

The restrictions places on the load impedances and the transmission line geometry for assuring a diagonal reflection coefficient are rather severe, so, in the actual case, it is to be expected that there will be mode conversion at the loads of the multiconductor line. In order to attempt to model the bulk current on a multiconductor line by a single line, it is useful to extract the bulk-bulk mode reflection coefficient from the $\bar{\bar{\rho}}$ matrix and then require that the single line model have the same reflection coefficient at the load.

For the special choice of the eigenmodes on the transmission line and the resulting $\bar{\bar{T}}$ matrix in Equation (61), the bulk mode reflection coefficient at a load is

given by the $i = 1$, $j = 1$ element of the reflection coefficient matrix, $\bar{\bar{\rho}}_\ell$. Denoting this reflection coefficient as $\rho_{\ell_{1,1}}$ and equating to the single line reflection coefficient of Equation (57), we obtain

$$\rho_\ell = \frac{Z_\ell - Z_c}{Z_\ell + Z_c} = \rho_{\ell_{1,1}} \tag{66}$$

where Z_ℓ and Z_c are the load impedance and characteristic impedance of the single wire line. This last equation may be solved for the single line load impedance as

$$Z_\ell = Z_c \frac{1 + \rho_{\ell_{1,1}}}{1 - \rho_{\ell_{1,1}}} \tag{67}$$

With Equation (67) the load impedance of the single wire transmission line is found in terms of the load and characteristic impedances of a multiconductor transmission line. It is still necessary, however, to determine an appropriate value for the single line characteristic impedance, Z_c.

On the single wire transmission line, the characteristic impedance relates voltage and current as

$$V^+(z) = Z_c I^+(z) \tag{68}$$

where the (+) sign refers to the forward propagating waves on the line. Since we wish the single line current $I(z)$ to behave similarly to the bulk current on the multiconductor line, $I_B(x)$, we can equate the forward propagating components as

$$I^+(z) = I_B^+(z) = \sum_{i=1}^{N} I_i^+(z) \tag{69}$$

where $I_i^+(z)$ represents the individual forward propagating components of the current on the i^{th} wire.

Similarly, we can define an appropriate single line forward propagating voltage, $V^+(x)$, by averaging over the elements of the multiconductor line voltage, $\overline{V}^+(z)$, as

$$V^+(z) = \frac{1}{N} \sum_{i=1}^{N} V_i^+(z) \tag{70}$$

With the forward propagating single line voltages and current thus defined, the single line characteristic impedance may be defined as

$$Z_C = \frac{V^+(z)}{I^+(z)} = \frac{\sum_{i=1}^{N} V_i^+(z)}{N \sum_{i=1}^{N} I_i^+(z)} \tag{71}$$

From Equations (43) and (48), the forward propagating multiconductor voltages and currents can be identified as

$$\bar{\bar{V}}^{+}(z) = \bar{\bar{Z}}_c \; \bar{\bar{T}} \; e^{-\bar{\bar{\gamma}}z} \; \bar{\alpha}^{+} \tag{72a}$$

and

$$\bar{\bar{I}}^{+}(z) = \bar{\bar{T}} \; e^{-\bar{\bar{\gamma}}z} \; \bar{\alpha}^{+} \tag{72b}$$

Thus, Equation (71) formally becomes

$$Z_c = \frac{\sum_{i=1}^{N} [\bar{\bar{Z}}_c \; \bar{\bar{T}} \; e^{-\bar{\bar{\gamma}}z} \; \bar{\alpha}^{+}]_i}{N \sum_{i=1}^{N} [\bar{\bar{T}} \; e^{-\bar{\bar{\gamma}}z} \; \bar{\alpha}^{+}]_i} \tag{73}$$

Note that this definition is rather undesirable, since there is a dependence on the line position z, as well as the mode excitation, $\bar{\alpha}^{+}$. Ideally, a characteristic impedance should not depend upon these parameters.

Considerable simplification results if it is possible to identify one mode which is the predominant bulk mode. Letting $\bar{\phi}_1$ be the bulk mode and γ_1^2 be its corresponding eigenvalue, Equation (73) can be simplified to give

$$Z_c = \frac{\left(\sum_{i=1}^{N} [\bar{\bar{Z}}_c \; \bar{\phi}_1]_i \right) e^{-\gamma_1 z} \; [\bar{\alpha}^{+}]_1}{N \left(\sum_{i=1}^{N} [\bar{\phi}_1]_i \right) e^{-\gamma_1 z} \; [\bar{\alpha}^{+}]_1} \tag{74}$$

since the sums of the other current modes $\bar{\phi}_j$ and voltage modes $\bar{\bar{Z}}_c \bar{\phi}_j$ are very small, because, by definition, they are differential modes which do not contribute to the bulk current.

In this last equation, it is now possible to eliminate the mode excitation term, $\vec{\alpha}^+$ and the exponential propagation term, since they are both scalars, to yield the following equation for the equivalent single line impedance:

$$Z_c = \frac{\sum_{i=1}^{N} [\bar{\bar{Z}}_c \bar{\phi}_1]_i}{N \sum_{i=1}^{N} [\bar{\phi}_1]_i} \tag{75}$$

If, as discussed previously, it is assumed that only single velocity waves propagate on the line, so that the current eigenmodes can be chosen to have the form given by Equation (61), the bulk mode $\bar{\phi}_1$ will then be a constant vector. If the characteristic impedance matrix has the form $Z_{c_{i,i}} = Z_1$ and $Z_{c_{i,j}} = Z_2$ which is a consequence of a random lay cable configuration, the single line characteristic impedance can then be expressed as

$$Z_c = \frac{Z_1 + (N-1)\, Z_2}{N} \tag{76}$$

which is simply the average of a row (or a column) of the multiconductor characteristic impedance matrix, $\bar{\bar{Z}}_c$.

As an example of a calculation using this bulk current concept, consider a seven-wire transmission line having a cross section shown in Figure 22. For this line configuration, the capacitive coefficient matrix $\overline{\overline{C}}$ as defined in refs. (12) and (13) and calculated by Chang (ref. 20) takes the following form:

$$C = 10^{-11} \times \begin{bmatrix} 5.54 & -.91 & -.91 & -.91 & -.91 & -.91 & -.91 \\ -.91 & 4.83 & -1.08 & -.02 & -.003 & -.02 & -.08 \\ -.91 & -1.08 & 4.83 & -1.08 & -.02 & -.003 & -.02 \\ -.91 & -.02 & -1.08 & 4.83 & -1.08 & -.02 & -.003 \\ -.91 & -.003 & -.02 & -1.08 & 4.83 & -1.08 & -.02 \\ -.91 & -.02 & -.003 & -.02 & -1.08 & 4.83 & -1.08 \\ -.91 & -.08 & -.02 & -.003 & -.02 & -1.08 & 4.83 \end{bmatrix} \text{ farads/meter}$$

The inductance matrix $\overline{\overline{L}}$ is calculated from the inverse of $\overline{\overline{C}}^{-1}$ via Equation (35) and assuming a propagation velocity of $v = c = 3 \times 10^8$ meters/sec, the $\overline{\overline{L}}$ matrix takes on the form:

---

20. Chang, S., T.K. Liu and F.M. Tesche, "Calculation of the Per-Unit-Length Capacitance Matrix for Shielded Insulated Wires," AFWL-TR-77-89, Air Force Weapons Laboratory, Kirtland Air Force Base, NM, April 1977.

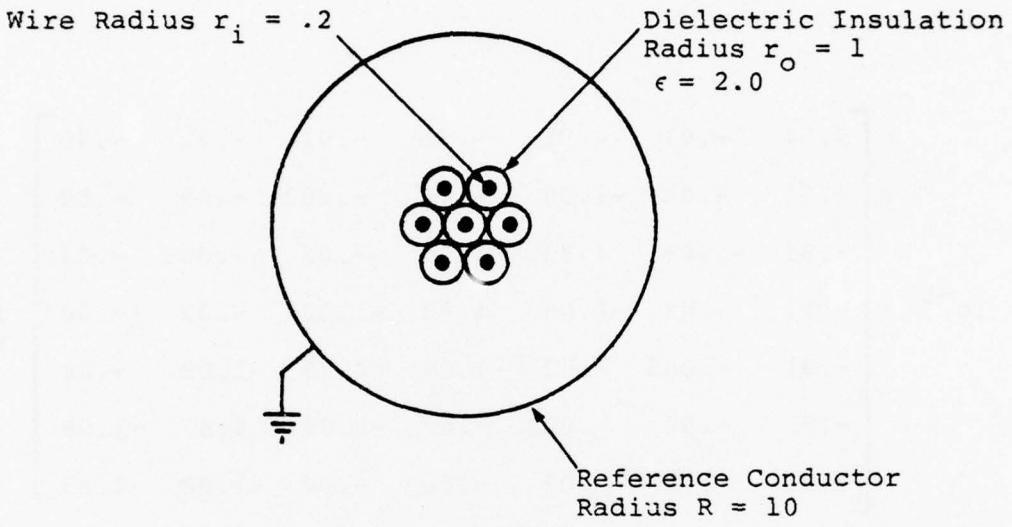

Figure 22. Cross Section of Seven Wire Transmission Line

$$L = 10^{-7} \times \begin{bmatrix} 3.04 & 1.05 & 1.05 & 1.05 & 1.05 & 1.05 & 1.05 \\ 1.05 & 2.93 & .97 & .53 & .44 & .53 & .97 \\ 1.05 & .97 & 2.93 & .97 & .53 & .44 & .53 \\ 1.05 & .53 & .97 & 2.93 & .97 & .53 & .44 \\ 1.05 & .44 & .53 & .97 & 2.93 & .97 & .53 \\ 1.05 & .53 & .44 & .53 & .97 & 2.93 & .97 \\ 1.05 & .97 & .53 & .44 & .53 & .97 & 2.93 \end{bmatrix} \text{ henrys/meter}$$

Note that the propagation velocity will be sightly slower than the velocity of light in free space due to the dielectric present around the wires. This effect, however, is neglected in this illustrative example.

The eigenvalues of $\overline{\overline{C}}\,\overline{\overline{L}}$ thus become

$$\gamma_i^2 = (s/3\times10^8)^2$$

for $i = 1$ to 7. Using the current eigenmodes defined by Equation (61), and assuming the load impedance to consist of 100 ohms from each wire to ground (i.e., $\overline{\overline{Z}}_\ell = 100\ \overline{\overline{U}}$), Equation (52) may be used to find the reflection matrix $\overline{\overline{\rho}}_\ell$. In this calculation, the characteristic impedance matrix $\overline{\overline{Z}}_c$ is found from Equation (47) to have the form

$$\bar{\bar{Z}}_c = \begin{bmatrix} 91.2 & 31.5 & 31.5 & 31.5 & 31.5 & 31.5 & 31.5 \\ 31.5 & 88.0 & 29.3 & 15.9 & 13.3 & 15.9 & 29.3 \\ 31.5 & 29.3 & 88.0 & 29.3 & 15.9 & 13.3 & 15.9 \\ 31.5 & 15.9 & 29.3 & 88.0 & 29.3 & 15.9 & 13.3 \\ 31.5 & 13.3 & 15.9 & 29.3 & 88.0 & 29.3 & 15.9 \\ 31.5 & 15.9 & 13.3 & 15.9 & 29.3 & 88.0 & 29.3 \\ 31.5 & 29.3 & 15.9 & 13.3 & 15.9 & 29.3 & 88.0 \end{bmatrix} \text{ ohms}$$

The result of these relatively simple calculations is the following reflection coefficient matrix at the load

$$\bar{\bar{\rho}}_\ell = \begin{bmatrix} -.39 & .12 & .12 & .12 & .12 & .12 & .12 \\ -.01 & .23 & -.04 & .06 & .07 & .06 & -.04 \\ -.01 & -.04 & .23 & -.04 & .06 & .07 & .06 \\ -.01 & .06 & -.04 & .23 & -.04 & .06 & .07 \\ -.01 & .07 & .06 & -.04 & .23 & -.04 & .06 \\ -.01 & .06 & .07 & .06 & -.04 & .23 & -.04 \\ -.01 & -.04 & .06 & .07 & .06 & -.04 & .23 \end{bmatrix}$$

Note that the magnitude of the bulk-bulk reflection coefficient $\rho_{\ell_{1,1}}$ is substantially larger than the other off diagonal terms in $\bar{\bar{\rho}}_\ell$. In addition, there is a high degree of symmetry in the matrix $\bar{\bar{\rho}}_\ell$, although it is not completely symmetric about the diagonal. Had another set of load impedances been chosen which consisted of a different impedance loading each wire, the symmetries found in $\bar{\bar{\rho}}_\ell$ would be less pronounced.

Since we are interested in the bulk-bulk reflection coefficient, it is interesting to compute $\overline{\overline{\rho}}_{\ell}$ under the assumptions that the multiconductor line randomly changes the individual wire locations. Averaging together the diagonal terms in the per-unit-length $\overline{\overline{C}}$ matrix and performing a similar average for the off-diagonal terms yields the following capacitive coefficient matrix

$$\overline{\overline{C}} = 10^{-11} \times \begin{bmatrix} 4.93 & -.57 & -.57 & -.57 & -.57 & -.57 & -.57 \\ -.57 & 4.93 & -.57 & -.57 & -.57 & -.57 & -.57 \\ -.57 & -.57 & 4.93 & -.57 & -.57 & -.57 & -.57 \\ -.57 & -.57 & -.57 & 4.93 & -.57 & -.57 & -.57 \\ -.57 & -.57 & -.57 & -.57 & 4.93 & -.57 & -.57 \\ -.57 & -.57 & -.57 & -.57 & -.57 & 4.93 & -.57 \\ -.57 & -.57 & -.57 & -.57 & -.57 & -.57 & 4.93 \end{bmatrix} \text{ farads/meter}$$

and the following characteristic impedance matrix:

$$\overline{\overline{Z}}_C = \begin{bmatrix} 83.8 & 23.3 & 23.3 & 23.3 & 23.3 & 23.3 & 23.3 \\ 23.2 & 83.8 & 23.3 & 23.3 & 23.3 & 23.3 & 23.3 \\ 23.3 & 23.3 & 83.8 & 23.3 & 23.3 & 23.3 & 23.3 \\ 23.3 & 23.3 & 23.3 & 83.8 & 23.3 & 23.3 & 23.3 \\ 23.3 & 23.3 & 23.3 & 23.3 & 83.8 & 23.3 & 23.3 \\ 23.3 & 23.3 & 23.3 & 23.3 & 23.3 & 83.8 & 23.3 \\ 23.3 & 23.3 & 23.3 & 23.3 & 23.3 & 23.3 & 83.8 \end{bmatrix} \text{ ohms}$$

Other types of averaging procedures can also be envisioned for this purpose. A detailed study of the best method for determining the average line properties has yet to be made.

Those, when combined with the previous $100\,\Omega$ load impedance matrix, yield the following reflection coefficient matrix

$$\overline{\overline{\rho}}_{\ell} = \begin{bmatrix} -.38 & & & & & & \\ & -.38 & & & & 0 & \\ & & -.38 & & & & \\ & & & -.38 & & & \\ & & & & -.38 & & \\ & 0 & & & & -.38 & \\ & & & & & & -.38 \end{bmatrix}$$

Notice that $\rho_{\ell_{1,1}}$ is almost identical to that for the controlled lay cable.

Using Equation (76) to define an appropriate single line impedance, we obtain

$$Z_c = \frac{Z_1 + (N-1)\, Z_2}{N} = \frac{83.8 + 6\times 23.3}{7} = 31.96 \text{ ohms}$$

The equivalent single line load is then directly computed from Equation (67) as

$$Z_{\ell} = Z_c \frac{1 + \rho_{\ell_{1,1}}}{1 - \rho_{\ell_{1,1}}} = 31.96 \ \frac{1 - .38}{1 + .38} = 14.29 \text{ ohms}$$

These values of Z_ℓ and Z_c are then used in the single line model to represent bulk current behavior on a multiconductor line.

As an example of the behavior of load currents in the time domain, the multiconductor line in Figure 21a was assumed to be excited with identical line voltages which had a unit step function time dependence. The transmission line length was ℓ = 1 meter and both the source and load impedances were taken as 100 ohms from the wires to ground. Figure 23 shows the transient behavior of the total ("bulk") current flowing into the load, as evaluated from Equation (59) and converted to the time domain using the fast Fourier transform (FFT).

A corresponding calculation was performed for the single line model using the characteristic impedance and load impedances defined above. The transient behavior for the single line load current was virtually indistinguishable from that of the multiconductor analysis, a fact not surprising in view of the symmetric excitation and loading of the line.

By changing one or more of the load impedances in $\overline{\overline{Z}}_\ell$, the reflection coefficient for the bulk current, $\rho_{\ell_{1,1}}$, and the single line load impedance, Z_c, will also change. For six wire loads fixed at 100 ohms and the

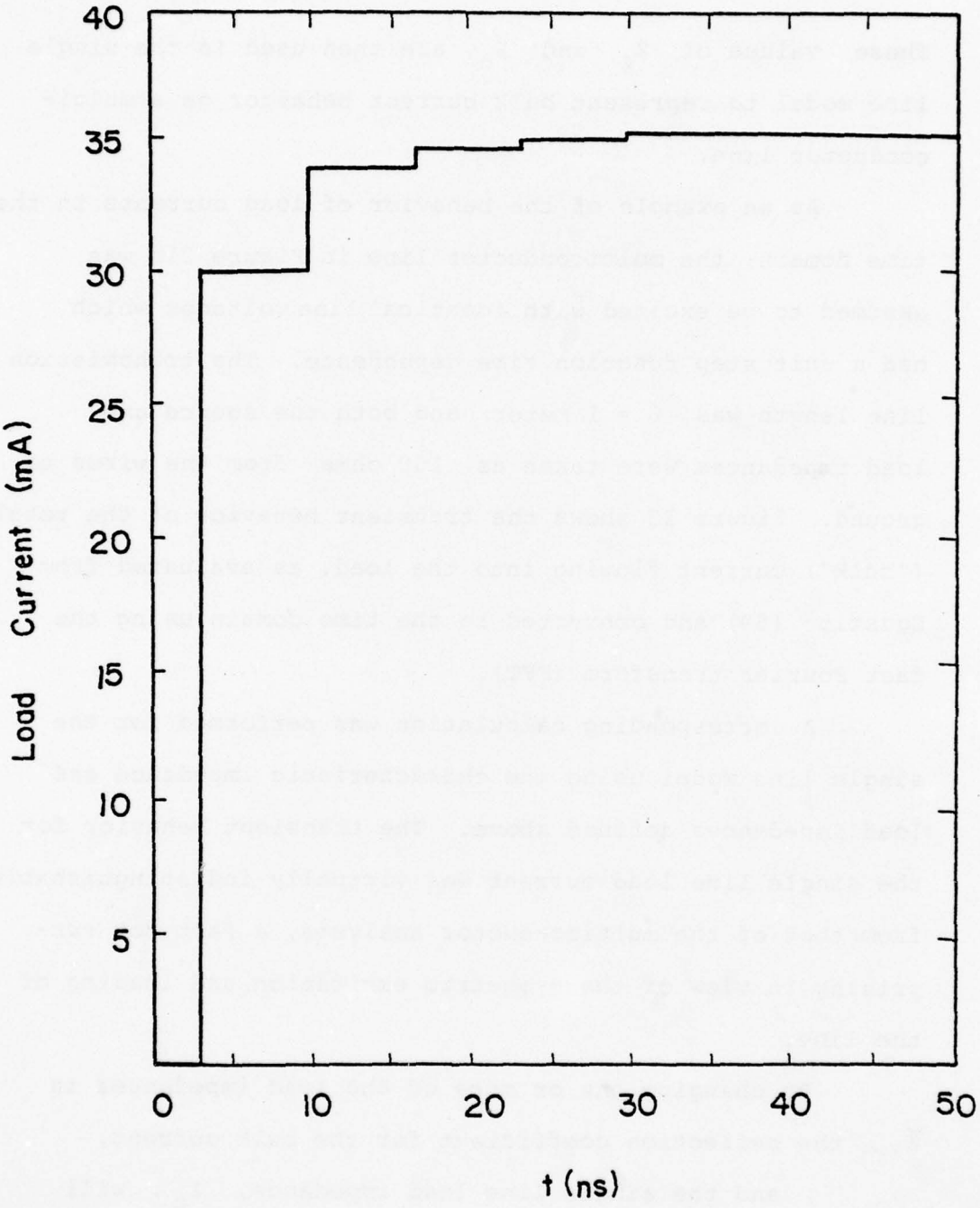

Figure 23. Step Function Response of Total Load Current of Multiconductor Line with L = 1 Meter and Source and Load Impedances of 100 Ω to Ground

seventh allowed to vary, Figure 24 shows the resulting reflection coefficient variation. Also plotted is the variation of the equivalent load impedance. These quantities are plotted as a function of the load impedance of wire #7, denoted by $Z_{\ell_{7,7}}$.

It is interesting to compare the transient response of the bulk current with the single line current of the load for the case of nonsymmetric loading. In Figure 25, this comparison is made for a load impedance of $Z_{\ell_{7,7}} = 1000\,\Omega$ on wire 7. The source impedance remained unchanged at $14.29\,\Omega$ for the single wire line and $\overline{\overline{Z}}_s = 100\,\overline{\overline{U}}$ for the multiconductor case. For this case, the effective single line impedance from Equation (67) is computed to be $Z_\ell = 16.47\,\Omega$.

Figure 26 shows similar results for a $1\,\Omega$ load on wire 7 of the multiconductor line. This corresponds to $Z_\ell = 10.0\,\Omega$ for the equivalent load.

From an examination of these last two figures, it may be seen that the single line model will predict the bulk response with an error of less than 10%. It must be emphasized, however, that these studies were performed with a step function excitation of idealized loads and a high degree of symmetry built into the analysis through the various assumptions employed. Additional studies with double exponential and damped sinusoid waveforms should be performed before it is possible to say with a good degree of certainty what the confidence levels are in this approach to bulk current modeling.

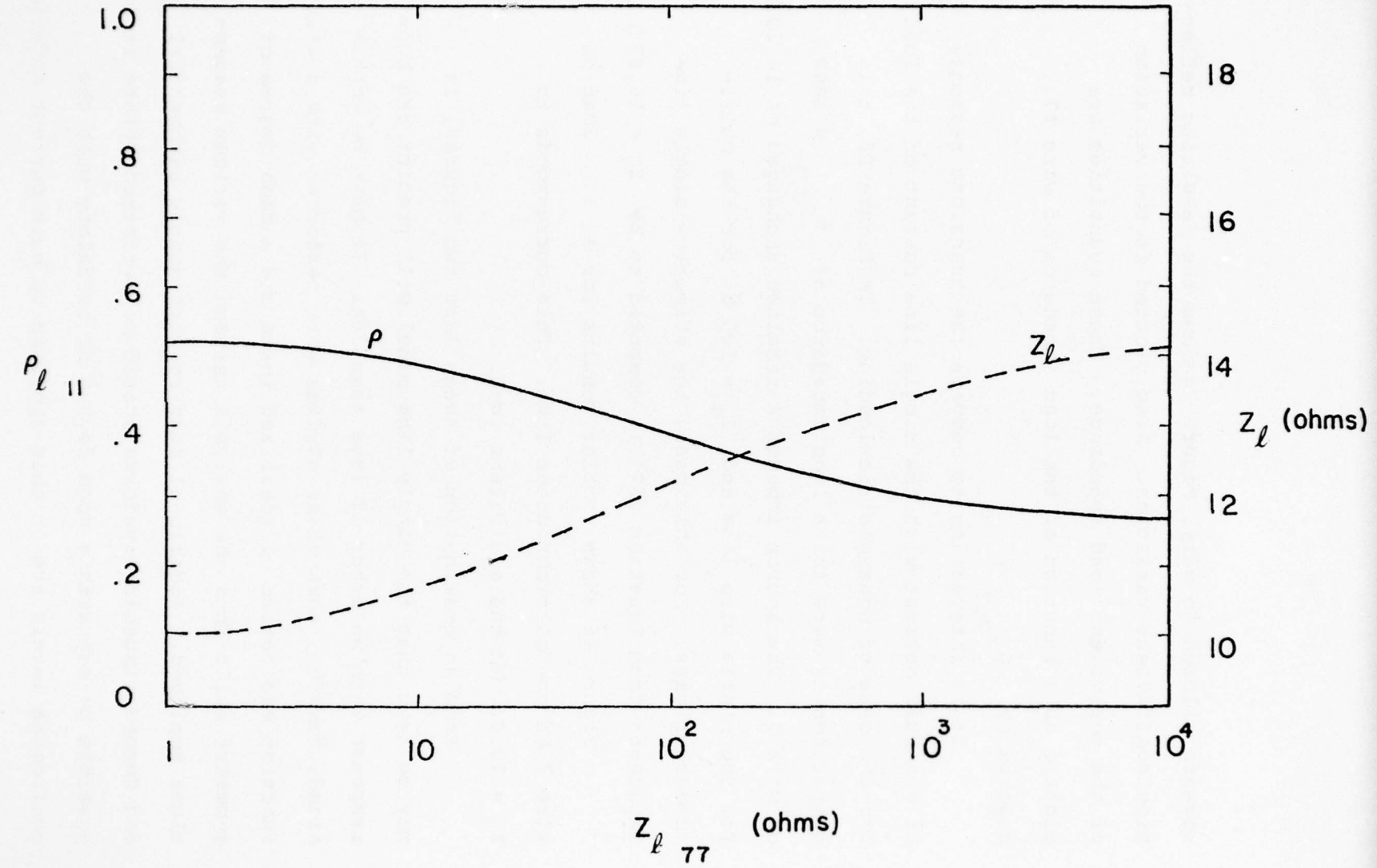

Figure 24. Variation of bulk mode reflection coefficient and resulting equivalent single line load impedance as a function of the load impedance on the seventh wire in the multiconductor bundle. All other multiconductor load impedances are 100 Ω to ground.

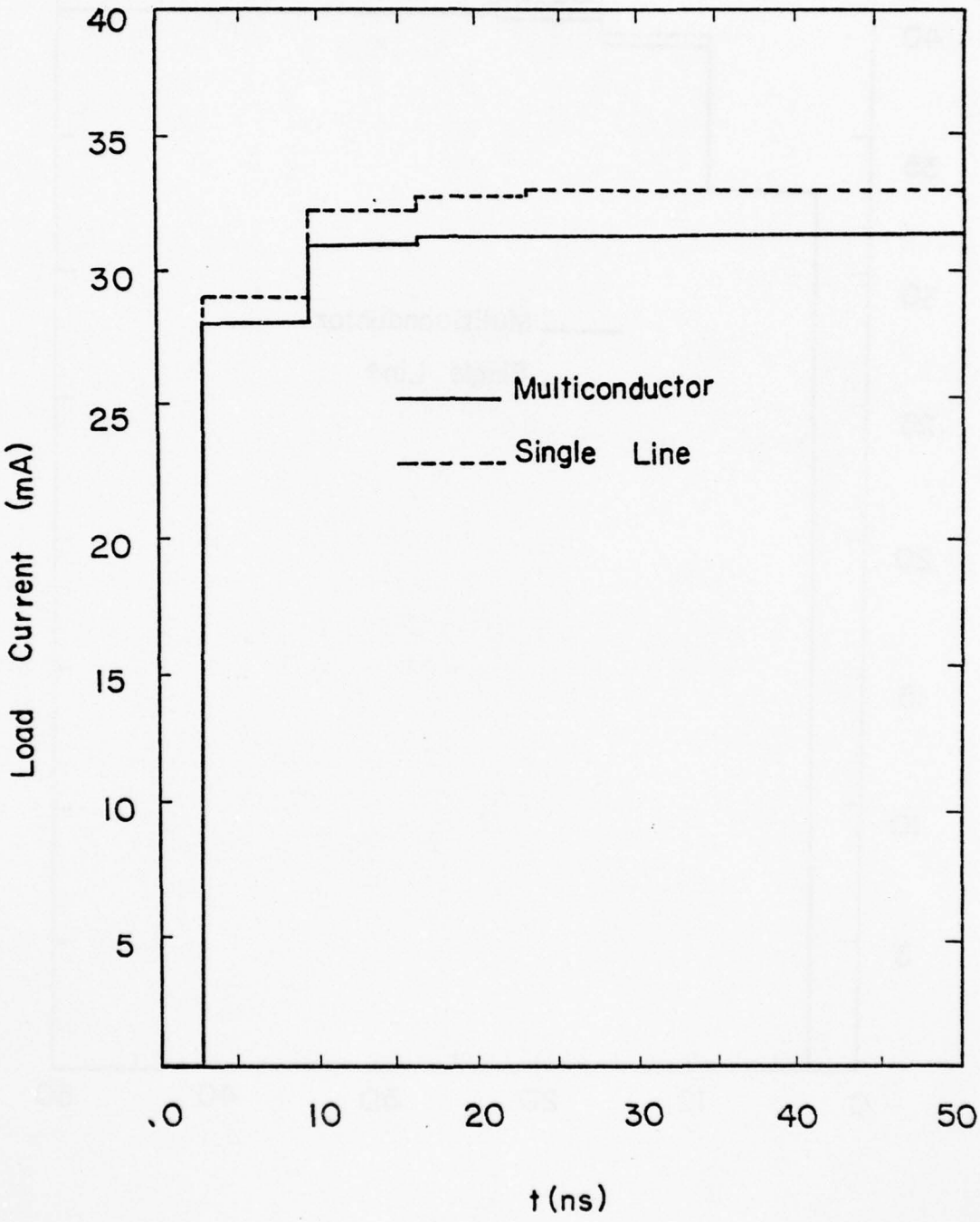

Figure 25. Comparison of Bulk Current and Single Wire Load Current for case of 1000 Ω load on Wire 7 and 100 Ω load on other wires.

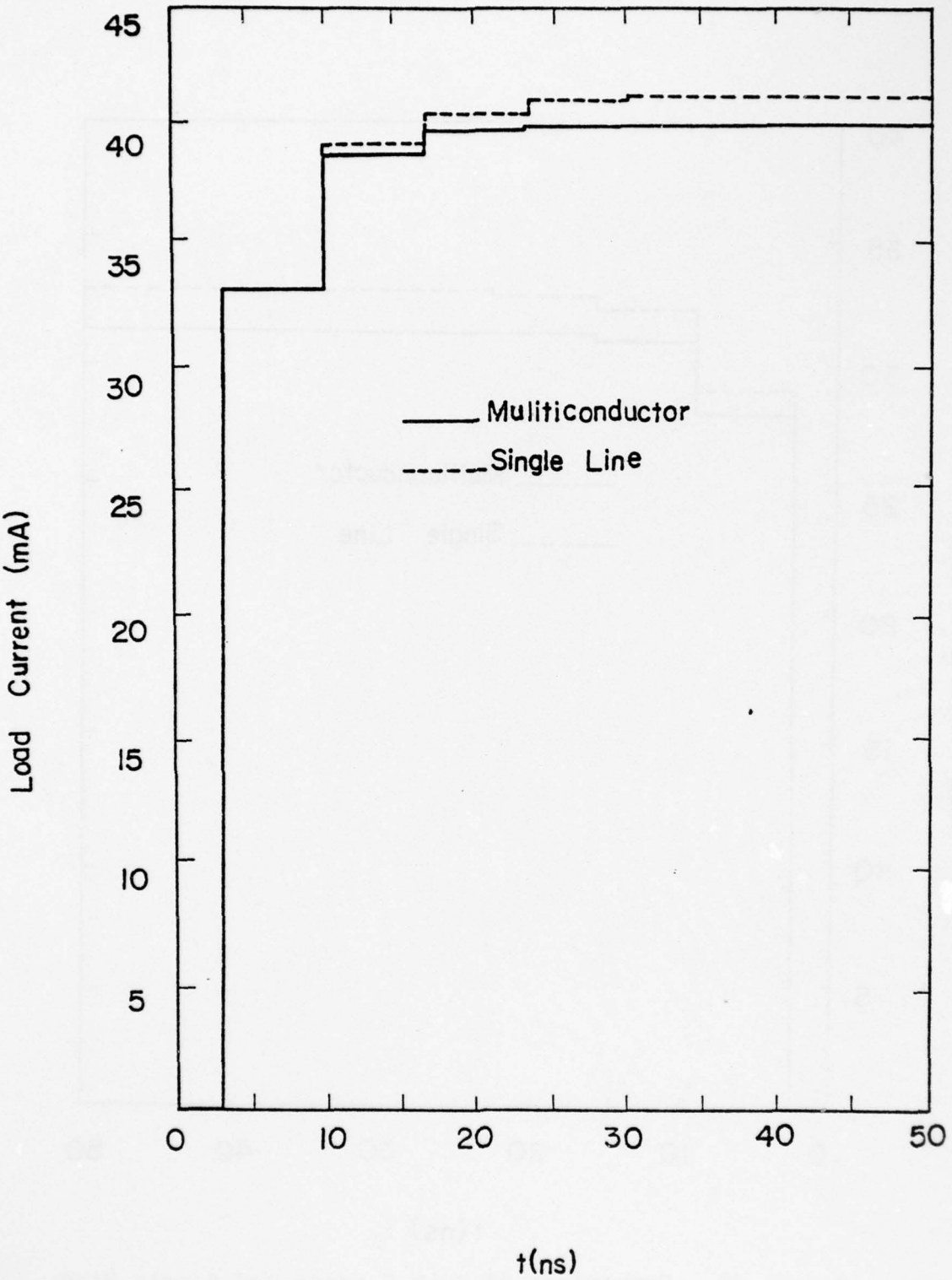

Figure 26. Comparison of Bulk Current and Single Wire Load Current for case of 1 Ω load on Wire 7 and 100 Ω load on other wires.

AD-A047 396 SCIENCE APPLICATIONS INC BERKELEY CALIF F/G 20/14
SELECTED TOPICS IN TRANSMISSION-LINE THEORY FOR EMP INTERNAL IN--ETC(U)
AUG 77 F M TESCHE, T K LIU F29601-76-C-0125

UNCLASSIFIED AFWL-TR-77-73 NL

2 OF 2
AD
A047396

END
DATE
FILMED
1 -78
DDC

SECTION V

CONCLUSION

This report has presented a number of improvements of single-wire transmission line theory for use in EMP internal interaction calculations. The case of a transmission line perturbation due to a nearby obstacle has been considered and various curves of the voltage reflection coefficient on the transmission line have been presented as a function of the equivalent line capacitance and inductance of the obstacle.

In addition, the effects of multiple loading due to two or more perturbing obstacles on a transmission line of finite length have been considered. Good agreement between the pass and stop bands calculated for this case and those of an infinite transmission line periodically loaded with similar obstacles has been observed. Both transient and time harmonic results for the load current on the periodically loaded, finite length transmission line have been computed for a typical transmission line having typical parameters.

Finally, we have investigated the possiblity of modeling the bulk current on a multiconductor transmission line by using a single-wire transmission line approximation and assuming that the total or "bulk" current on the multi-conductor line has the same reflection coefficient as does the current on the single-wire transmission line. Using this

approach, it is possible to determine an equivalent single-line characteristic impedance and single-line load impedance for the approximate model. Comparisons of the bulk current response and the single-wire current response for a step function excitation have been presented and the agreeement is reasonable. The responses for a damped sine and double exponential waveform still need to be studied.

REFERENCES

1. Tesche, F.M., et al., "Internal Interaction Analysis: Topological Concepts and Needed Model Improvements," AFWL-TR-75-282, Air Force Weapons Laboratory, Kirtland Air Force Base, NM, October 1975.

2. Tesche, F.M., et al., "Evaluation of Present Internal EMP Interaction Technology: Description of Needed Improvements," AFWL-TR-75-288, Air Force Weapons Laboratory, Kirtland Air Force Base, NM, October 1975.

3. Boeing Aircraft Corporation, "Common Mode Model Development for Complex Cable Systems," Boeing Report D224-10015-4, June 19, 1973.

4. Tesche, F.M., and T.K. Liu, "An Electric Model for a Cable Clamp on a Single Wire Transmission Line," AFWL-TR-76-325, Air Force Weapons Laboratory, Kirtland Air Force Base, NM, December 1976.

5. Coen, S., T.K. Liu and F.M. Tesche, "Calculation of the Equivalent Capacitance of a Rib near a Single-Wire Transmission Line," AFWL-TR-77-60, Air Force Weapons Laboratory, Kirtland Air Force Base, NM, February 1977.

6. Lee, K.S.H., and F.C. Yang, "A Wire Passing by a Circular Aperture in an Infinite Ground Plane," AFWL-TR-77-52, Air Force Weapons Laboratory, Kirtland Air Force Base, NM, June 1977.

7. Lam, J., "Equivalent Lumped Parameters for a Bend in a Two-Wire Transmission Line," AFWL-TR-77-5, Air Force Weapons Laboratory, Kirtland Air Force Base, NM, January 1977.

8. Lam, J., "Propagation Characteristics of a Periodically Loaded Transmission Line," AFWL-TR-76-324, Air Force Weapons Laboratory, Kirtland Air Force Base, NM, December 1976.

9. Ramo, S., and J. Whinnery, Fields and Waves in Modern Radio, John Wiley & Sons, New York, 1964.

10. Seshu, S., and N. Balabanian, Linear Network Analysis, John Wiley & Sons, New York, 1959.

11. King, R.W.P., Transmission-Line Theory, Dover, 1965.

12. Kajfez, D., "Multi-Conductor Transmission Lines," EMP Interaction Note Series, Note 151, Air Force Weapons Laboratory, Kirtland Air Force Base, NM, June 1972.

13. Liu, T., "Electromagnetic Coupling between Multiconductor Transmission Lines in a Homogeneous Medium," AFWL-TR-76-333, Air Force Weapons Laboratory, Kirtland Air Force Base, NM.

14. Paul, C.R., "On Uniform Multimode Transmission Lines," IEEE Trans. M.T.T., Vol. MTT-21, No. 8, August 1973, pp. 556-558.

15. Paul, C.R., "Efficient Numerical Computation of the Frequency Response of Cables Illuminated by an Electromagnetic Field," IEEE Trans. M.T.T., Vol. MTT-52, No. 4, April 1974, pp. 454-457.

16. Paul, C.R., "Useful Matrix Chain Parameter Identities for the Analysis of Multiconductor Transmission Lines," IEEE Trans. M.T.T., September 1975, pp. 756-760.

17. Frankel, S., Cable and Multi-Conductor Transmission Analysis, Harry Diamond Laboratories, HDL-TR-091-1, June 1974.

18. C.E. Baum, T.K. Liu, F.M. Tesche and S.K. Chang, "Numerical Results for Multiconductor Transmission-Line Networks," AFWL-TR-77-123 , Air Force Weapons Laboratory, Kirtland Air Force Base, NM, June 1977.

19. Morgan, M.A., and F.M. Tesche,"Statistical Analysis of Critical Load Excitations Induced on a Random Cable System by an Incident Driving Field: Basic Concepts and Methodology," AFWL-TR-75-281, Air Force Weapons Laboratory, Kirtland Air Force Base, NM, July 1975.

20. Chang, S., T.K. Liu and F.M. Tesche, "Calculation of the Per-Unit-Length Capacitance Matrix for Shielded Insulated Wires," AFWL-TR-77-89, Air Force Weapons Laboratory, Kirtland Air Force Base, NM, April 1977.